



ISAS - INTERNATIONAL SCHOOL FOR ADVANCED STUDIES



Scuola Internazionale Superiore di Studi Avanzati
International School for Advanced Studies

A statistical mechanics study of a prototype random combinatorial problem

Thesis submitted for the degree of
Magister Philosophiæ

Candidate:
Michele Leone

Supervisors:
Prof. Amos Maritan
Dott. Riccardo Zecchina

October 2000



Scuola Internazionale Superiore di Studi Avanzati
International School for Advanced Studies

A statistical mechanics study of a prototype random combinatorial problem

Thesis submitted for the degree of
Magister Philosophiæ

Candidate:
Michele Leone

Supervisors:
Prof. Amos Maritan
Dott. Riccardo Zecchina

October 2000

Contents

Preface	3
1 The 3-XOR-SAT Problem	7
1.1 Introduction	7
1.2 Mathematical description of the model	7
1.3 Outline of main results	10
1.4 Statistical mechanics analysis: the replica results	11
1.5 Connection with graph theory	15
1.6 Numerical results	18
1.7 Conclusions	26
2 The 2+p-XOR-SAT variant	29
2.1 Introduction: the role of phase coexistence and finite-size scaling .	29
2.2 Model definition and outline of some results	31
2.3 Statistical mechanics analysis	32
2.4 Numerical simulations	34
2.5 Conclusions and perspectives	41
Bibliography	44

Preface

Complexity theory [1], as arising from Cook's theorem of 1971 [2], deals with the issue of classifying combinatorial optimization problems according to the computational cost required for their solution. The hard problems are grouped in a class named NP, where NP stands for 'non-deterministic polynomial time'. These problems are such that a potential solution can be checked rapidly whereas finding one solution may require an exponential time in the worst case. In turn, the hardest problems in NP belong to a sub-class called NP-complete which is at the root of computational complexity. The completeness property refers to the fact that if an efficient algorithm for solving just one of these problems could be found, then one would have an efficient algorithm for solving all problems in NP. By now, a huge number of NP-complete problems have been identified [1], and the lack of an efficient algorithm corroborates the widespread conjecture that $NP \neq P$, i.e. that no such algorithm exists.

Complexity theory is based on a worst-case analysis and therefore does not depend on the properties of the particular instances of the problems under consideration. In order to deepen the understanding of typical-case complexity rather than the worst-case one and to improve and test algorithms for real world applications, computer scientists have recently focused their attention on the study of random instances of hard computational problems, seeking for a link between the onset of computational complexity and some intrinsic (i.e. algorithm independent) properties of the model. Analytical and numerical results have accumulated [3, 39, 5, 38, 7] showing that the computationally hard instances appear with a significant probability only when generated near "phase boundaries", i.e. when problems are critically constrained. Such phenomenon is known as the easy-hard transition.

Randomized search algorithms provide efficient heuristics for quickly finding solutions provided they exist. At the phase boundary, however, there appears an exponential critical slowing down which makes the search inefficient for any practical purpose. Understanding the behaviour of search processes at the easy-hard transition point constitutes an important theoretical challenge which can be viewed as the problem of building a generalized off-equilibrium theory for stochastic processes which do not satisfy detailed balance. No static probability measure, *à la* Gibbs, describing the asymptotic statistical behaviour of the search

processes is guaranteed to exist. Moreover, the hardest random instances of combinatorial optimization problems provide a natural test-bed for the optimization of heuristic search algorithms which are widely used in practice.

How to generate hard and solvable instances is far from obvious and very few examples of such generators are known [9]. In most cases, like e.g. in the random Boolean Satisfiability problem (K-SAT [38, 7, 45], hard instances can be only found in a very narrow region of the parameters space. In this region the probability that a random instance of the problem has no solution at all is finite. Then, heuristic (incomplete) search algorithms have no way to disentangle, in a given finite time, the unsatisfiable instances, from those which are simply very hard to solve.

In this paper, we shall discuss a very simple and exactly solvable model for the generation of random combinatorial problems. On the one hand, such problems become extraordinarily hard to solve by local search methods in a large region of the parameter space and yet at least one solution may be superimposed by construction. On the other hand, the model may be solved in polynomial time by a simple global method and therefore belongs to the class P.

At variance with respect to the famous random 2-SAT problem [11, 45], which is in P and can be solved efficiently by local search methods [12] also at the phase boundary, the model we consider undergoes an easy-hard transition very similar (even harder) to the one observed in 3-SAT as far as local search methods is concerned. However, the exact mapping of the model on a minimization problem over uniform random hyper-graphs makes the problem analytically tractable and also solvable in polynomial time by global methods which allows for the numerical study of very large systems. Therefore, some of the open questions which arise in the analysis of 3-SAT and which are common to the present model can be answered exactly.

In the context of statistical physics the model provides a simple model for the glass transition, in which the crystalline state can be viewed as the superimposed solution and the structure of the excited states is responsible for the off-equilibrium behaviour and the associated structural glass transition. These aspects will be the subject of a forthcoming paper. The limit of infinite connectivity provides one of the most studied models in the context of spin glass theory, see for instance [13, 14, 15, 16, 17, 18].

Chapter 1

The 3-XOR-SAT Problem

1.1 Introduction

In the first part of this work we study a simple and exactly solvable model for the generation of random combinatorial problems, which is a diluted p-spin model at zero temperature in the statistical mechanics language. While such problems become extraordinarily hard to solve by local search methods in a large region of the parameter space, still at least one solution may be superimposed by construction. The statistical properties of the model can be studied exactly by the replica method and each single instance can be analyzed in polynomial time by a simple global solution method. The geometrical/topological structures responsible for dynamic and static phase transitions as well as for the onset of computational complexity in local search method are thoroughly analyzed. Numerical analysis on very large samples allows for a precise characterization of the critical scaling behaviour.

1.2 Mathematical description of the model

In order to unveil the different aspects of the model, to be referred to as *hyper-SAT* (hSAT), we give explicitly its definition both as a satisfiability problem and as a minimization problem over hyper-graphs.

Here we discuss the hSAT model with $K = 3$ variables per constraint, which can be viewed as a perfectly balanced version of the famous random 3-SAT problem. The case $K = 2$ does not present any interesting computational features as far as hardness is concerned because it can be solved efficiently both by local and global methods. Generalizations to $K > 3$ are straightforward.

Given a set of N Boolean variables $\{x_i = 0, 1\}_{i=1, \dots, N}$, we construct an instance of 3-hSAT as follows. Firstly we define the following elementary constraints (4-clauses sets with 50% satisfying assignments)

$$\begin{aligned}
C(ijk|+1) &= (x_i \vee x_j \vee x_k) \wedge (x_i \vee \bar{x}_j \vee \bar{x}_k) \\
&\quad \wedge (\bar{x}_i \vee x_j \vee \bar{x}_k) \wedge (\bar{x}_i \vee \bar{x}_j \vee x_k) \\
C(ijk|-1) &= (\bar{x}_i \vee \bar{x}_j \vee \bar{x}_k) \wedge (\bar{x}_i \vee x_j \vee x_k) \\
&\quad \wedge (x_i \vee \bar{x}_j \vee x_k) \wedge (x_i \vee x_j \vee \bar{x}_k) ,
\end{aligned} \tag{1.1}$$

where \wedge and \vee stand for the logical AND and OR operations respectively and the over-bar is the logical negation. Then, by randomly choosing a set E of M triples $\{i, j, k\}$ among the N possible indices and M associated unbiased and independent random variables $J_{ijk} = \pm 1$, we construct a Boolean expression in Conjunctive Normal Form (CNF) as

$$F = \bigwedge_{\{i,j,k\} \in E} C(ijk|J_{ijk}) . \tag{1.2}$$

A logical assignment of the $\{x_i\}$'s satisfying all clauses, that is evaluating F to true, is called a solution of the 3-hSAT problem. If no such assignment exists, F is said to be unsatisfiable.

A slightly different choice of J_{ijk} allows to construct hSAT formulæ which are random but guaranteed to be satisfiable. To every Boolean variable we associate independently drawn random variables $\varepsilon_i = \pm 1$, and define $J_{ijk} = \varepsilon_i \varepsilon_j \varepsilon_k$ for all $\{i, j, k\} \in E$. For this choice, CNF formula in Eq.(2.3) is satisfied by $\{x_i \mid x_i = +1 \text{ if } \varepsilon_i = +1, x_i = 0 \text{ if } \varepsilon_i = -1\}$. As we shall discuss in great detail, these formulæ provide a uniform ensemble of hard satisfiable instances for local search methods. We refer to this version of the model as the *satisfiable hSAT*. Indeed, the random signs of J_{ijk} can be removed in this satisfiable case by negating all Boolean variables x_i associated to negative ε_i . The resulting model has $J_{ijk} = +1$ for all $\{i, j, k\} \in E$, and the forced satisfying solution is $x_i = 1, \forall i = 1, \dots, N$. The use of the $\{\varepsilon_i\}$ is a way of hiding the latter solution by a *random gauge transformation* without changing the properties of the model. The impossibility of inverting efficiently the gauge transformation by local methods is a consequence of the branching process arising from the presence of $K = 3$ variables in each constraint. For any $K > 3$ the same result would hold whereas for $K = 2$ the problem trivializes.

The hSAT model can be easily described as a minimization problem of a cost-energy function over a random hyper-graph. Given a random hyper-graph $\mathcal{G}_{N,M} = (V, E)$, where V is the set of N vertices and E is the set of M hyper-edges joining triples of vertices, the energy function to be minimized reads

$$H_J[\mathbf{S}] = M - \sum_{\{i,j,k\} \in E} J_{ijk} S_i S_j S_k , \tag{1.3}$$

where each vertex i bears a binary “spin” variable $S_i = \pm 1$, and the weights J_{ijk} associated to the random bonds can be either ± 1 at random, in the so called *frustrated* case, or simply equal to 1 in the *unfrustrated* model.

Once the mapping $S_i = 1$ if $x_i = 1$ and $S_i = -1$ if $x_i = 0$ is established, one can easily notice that the energy function in Eq.(2.4) simply counts the number of violated clauses in the previously defined CNF formulæ with the same set of J 's. The frustrated and the unfrustrated cases correspond to the hSAT and to the satisfiable hSAT formulæ respectively.

The computational issue consists in finding a configuration of spin variables which minimizes H . If all the terms $J_{ijk}S_iS_jS_k$ appearing in the energy are simultaneously maximized ("satisfied") the energy vanishes. This is always possible in the unfrustrated case just by setting $S_i = 1, \forall i$. In the frustrated case, there exist a critical value of the average connectivity above which the various terms start to be in conflict, that is frustration becomes effective in the model. In random hyper-graphs the control parameter is the average density of bonds, $\gamma = M/N$ (or, for the CNF formula, the density of clauses $\alpha = 4\gamma$). For sufficiently small densities, the graph consists of many small connected clusters of size up to $O(\ln N)$. If γ increases up to the percolation value $\gamma_p = 1/6$, there appears a spanning cluster containing a finite fraction of the N sites in the limit of large N . However, such a spanning cluster can a priori have a tree-like structure, for which the randomness of the couplings $J_{ijk} = \pm 1$ can be eliminated by a proper gauge transformation, $S_i \rightarrow \pm S'_i$, of the spin variables. As we shall see, there exist two other thresholds of the bond density at which more complicated and interesting dynamical and structural changes take place.

In spite of apparent similarities, hSAT and the random Boolean Satisfiability problem (K-SAT [19]) differ in some basic aspects.

In K-SAT the fluctuations of the frequencies of appearance of the variables in the clauses lead to both single and two body interactions in the associated energy function [20] which force the minima in some specific random directions and which rule out the existence of a purely dynamical threshold (see below). Algorithms may take advantage of such information and both heuristic as well as complete algorithms show a performance which indeed depends on the criterion used to fix the variables. For example, rigorous lower bounds to the critical threshold have been improved recently by exploiting this opportunity in a simple tractable way [21]. On the same footing, the efficiency of the most popular heuristic and complete search algorithms, namely walk-sat [22] and TABLEAU [23], is again based on strategies which exploit the above structure. Note that the above improvements can not be applied to the hSAT model where formulæ are completely balanced.

Moreover, in K-SAT the mapping of the problem over directed random graphs is rather involved and the exact analytical solution is still lacking, while in hSAT the connection to random hyper-graphs is clear and makes the analysis tractable.

Finally, restriction of K-SAT to satisfiable instances (for instance by selecting at random clauses which are satisfied by a previously fixed assignment of variables) does not provide a uniform ensemble of hard satisfiable problems even when restricted to local search methods [24].

Given the mapping over random hyper-graphs, the satisfiability problem for hSAT can be solved in $O(N^3)$ steps by simply noticing that the problem of satisfying all constraints is nothing but the problem of solving an associated linear system modulo 2, i.e. in $GF[2]$. Upon introducing the two sets of binary variables $\{a_i\} \in \{0, 1\}^N$ and $\{b_{ijk}\} \in \{0, 1\}^M$ such that $(-1)^{a_i} = S_i$ and $(-1)^{b_{ijk}} = J_{ijk}$, the hSAT decision problem becomes simply the problem of determining the existence of a solution in $GF[2]$ to the random linear system $a_i + a_j + a_k = b_{ijk}$, with ijk running over all triples.

Finally, we notice that in the high γ UNSAT (or frustrated) region the optimization problem of minimizing the number of violated constraints, the so called MAX-hSAT, is indeed computationally very hard both for complete and incomplete algorithms and no global method for finding ground states is available.

1.3 Outline of main results

For the sake of clarity, we anticipate here the main results leaving for the following sections a thorough discussion of the analytical and numerical studies.

The frustrated hSAT model presents two clear transitions. The first one appears at $\gamma_d = 0.818$ and it is of purely dynamical nature. There the typical formula still remains satisfiable with probability one, but an exponential number of local energy minima appear at positive energies. Deterministic algorithms, like greedy search or zero temperature dynamics, try to decrease the energy in every step and thus get stuck at least at this threshold. Randomized algorithms may escape from these minima, but they undergo a slowing down from an exponentially fast convergence to a polynomially slow one, i.e. at γ_d the typical time for finding a solution diverges as a power of the number of variables. The dynamical transition at γ_d seems to be accompanied by a dynamical glassy transition due to replica symmetry breaking (RSB) effects connected with the appearance of an exponential number of local minima. An approximate variational calculation (see ref. [43] for a discussion on the method) involving RSB gives $\gamma_{d,rsb}^{var} \simeq 0.83$ which is in good agreement with the value of γ_d where local minima appear.

The second transition appears at $\gamma_c = 0.918$ and corresponds to the so called SAT/UNSAT transition (below γ_c the typical problem is satisfiable whereas above γ_c it becomes unsatisfiable). At this point the structure of the global energy minima changes abruptly. The ground states have strictly positive energy, thus no satisfying assignments for the hSAT formula exist any more. While the number of these configurations is always exponentially large (the ground state entropy is always finite), at γ_c a finite fraction of the variables, the so-called *backbone* component, becomes totally constraint, i.e. the backbone variables take the same value in all minima [26]. An important difference of the SAT/UNSAT transition in hSAT compared to K-SAT [43] is the non-existence of any precursor. For $\gamma < \gamma_c$ and large N , all variables S_i take equally often the values $+1$ and -1 in

the ground states (they have zero local magnetization), even those which become backbone elements when γ_c is reached by adding new 4-clauses sets. The lack of any precursor comes from the non-existence of single- or two-body interactions in Eq.(2.4).

The unfrustrated or satisfiable hSAT problem has by construction at least one solution which we find to be superimposed without affecting the statistical features of the model for $\gamma < \gamma_c$ in the limit of large N , including the dynamical transition at $\gamma_d = 0.818$. It is impossible to get any information on the superimposed solution by looking at the full solution space, because it is completely hidden by the exponential number of ground states. Randomly chosen satisfying assignments do not show any correlation. At exactly the same $\gamma_c = 0.918$ as in the frustrated model, there appears a transition from a SAT phase with exponentially many unbiased solutions to another SAT phase where the solutions are strongly concentrated around the superimposed solution. The latter one is now hidden by the presence of exponentially many local energy minima with positive cost. These minima have exactly the statistical properties of the global minima of the corresponding frustrated hSAT problem, that is the hSAT problem defined over the same hyper-graph but with randomized signs of the couplings J_{ijk} . More specifically, the energy, the entropy and the backbone component size coincide. Due to their finite entropy, an algorithm will thus hit many of these local minima before it reaches the satisfying ground state. As one can see from Fig. 1.5, finding this solution by backtracking, e.g. with the Davis-Putnam (DP) procedure [27], is nevertheless easier than proving the unsatisfiability of hSAT (or identifying ground states in the frustrated version). This results stems from the missing information on the true ground state energy of hSAT above γ_c . The solution time is however found to be clearly exponential in both cases. In the $\gamma \geq \gamma_c$ region, the model provides a uniform ensemble of hard SAT instances for local methods which can be used to test and optimize algorithms.

1.4 Statistical mechanics analysis: the replica results

In our analytical approach, we exploit the well known analogies between combinatorial optimization problems and statistical mechanics. In both cases, the system is characterized by some cost-energy function, as it is given e.g. by Eq.(2.4) for hSAT. In equilibrium statistical mechanics, any configuration $\mathbf{S} = \{S_i\}_{i=1\dots N}$ is realized with probability $\exp\{-\beta H[\mathbf{S}]\}/Z$ where $\beta = 1/T$ is the inverse temperature and Z the partition function. If the temperature is lowered, the probability becomes more and more concentrated on the global energy minima and finally, for $T = 0$, only the ground states keep non-zero weights. In order to compute the average free energy, we resort to the replica symmetric (RS) functional replica

method developed for diluted spin glasses which is known to provide exact results for ferromagnetic models.

The calculation of the average value of the logarithm of Z is in general impossible. To circumvent this difficulty, we compute the n^{th} moment of Z for integer-valued n and perform an analytical continuation to real n to exploit the identity $\log \ll Z^n \gg = 1 + n \ll \log Z \gg + O(n^2)$. The n^{th} moment of Z is obtained by replicating n times the sum over the spin configuration and averaging over the disorder [44]

$$\ll Z^n \gg = \sum_{\mathbf{S}^1, \mathbf{S}^2, \dots, \mathbf{S}^n} \ll \exp \left(-\beta \sum_{a=1}^n H_J[\mathbf{S}^a] \right) \gg, \quad (1.4)$$

which in turn may be viewed as a generating function in the variable $\exp(-\beta)$.

In order to compute the expectation values that appear in Eq.(2.5), one notices that each single term $\exp(-\beta \sum_{a=1}^n H_J[\mathbf{S}^a])$ factorises over the sets of different triples of indices due to the absence of any correlation in the probability distribution of the J_{ijk} . It follows

$$\ll Z^n \gg = \sum_{S_i^1, S_i^2, \dots, S_i^n} \ll \exp \left\{ -\beta \gamma N n - \gamma N + \frac{\gamma}{N^2} \sum_{ijk} e^{\beta \sum_a S_i^a S_j^a S_k^a} + O(1) \right\} \gg \quad (1.5)$$

The averaged term in Eq.(2.7) depends on the $n \times N$ spin replicas only through the 2^n occupation fractions $c(\vec{\sigma})$ labelled by the vectors $\vec{\sigma}$ with n binary components; $c(\vec{\sigma})$ equals the number (divided by N) of labels i such that $S_i^a = \sigma^a$, $\forall a = 1, \dots, n$. Therefore, the final expression of the n^{th} moment of Z to the leading order in N (i.e. by resorting to a saddle point integration), can be written as $\ll Z^n \gg \simeq \exp(N F[c])$ where $F[c]$ is the maximum over all possible $c(\vec{\sigma})$'s of the functional [44]

$$-\beta F[c] = -\gamma(1 + \beta n) - \sum_{\vec{\sigma}} c(\vec{\sigma}) \log c(\vec{\sigma}) + \gamma \sum_{\vec{\sigma}, \vec{\rho}, \vec{\tau}} c(\vec{\sigma}) c(\vec{\rho}) c(\vec{\tau}) \exp(\beta \sum_a \sigma^a \rho^a \tau^a) \quad (1.6)$$

The saddle point equation $\frac{\partial(-\beta F)}{\partial c(\vec{\sigma})} = 0$ reads

$$c(\vec{\sigma}) = \exp \left\{ -\Lambda + 3\gamma \sum_{\vec{\rho}, \vec{\tau}} c(\vec{\rho}) c(\vec{\tau}) \exp(\beta \sum_a \sigma^a \rho^a \tau^a) \right\} \quad (1.7)$$

where the Lagrange multiplier $\Lambda = 3\gamma$ enforces the normalization constraint $\sum_{\vec{\sigma}} c(\vec{\sigma}) = 1$. In Eq.(1.6), one may easily identify two terms, one model dependent and the other $(-\sum_{\vec{\sigma}} c(\vec{\sigma}) \log c(\vec{\sigma}))$ simply describing the degeneracy (the so called combinatorial *entropy*) with which each term of the generating function appears given the representation in terms of the occupation fractions. In the limit of interest $T \rightarrow 0$ and in the Replica Symmetric subspace, the freezing of the spin

variables is properly described by a rescaling of the local magnetizations of the form $m = \tanh(h/T)$. The probability distribution $P(h)$ of the h 's is therefore introduced through the generating functional

$$c(\vec{\sigma}) \int_{-\infty}^{\infty} P(h) \frac{e^{\beta h \sum_a \sigma^a}}{(2 \cosh(\beta h))^n} \quad (1.8)$$

where h is nothing but an effective field in which the spins are immersed. In this representation, the free-energy reads

$$\begin{aligned} -\beta F[P(h)] = & \\ \gamma \int dh_1 dh_2 dh_3 P(h_1) P(h_2) P(h_3) \log T(h_1, h_2, h_3, \beta) & \\ + \int \frac{dh dK}{2\pi} e^{-ihK} P_{FT}(K) [1 - \log P_{FT}(K)] \log[2 \cosh(\beta h)] & \end{aligned} \quad (1.9)$$

where $P_{FT}(K)$ is the Fourier Transform of $P(h)$ and

$$T = \frac{2 \cosh(\beta(h_1 + h_2)) [e^{\beta h_3} + e^{-2\beta - \beta h_3}] + 2 \cosh(\beta(h_1 - h_2)) [e^{-\beta h_3} + e^{-2\beta + \beta h_3}]}{(2 \cosh(\beta h_1)) (2 \cosh(\beta h_2)) (2 \cosh(\beta h_3))} \quad (1.10)$$

The associated saddle-point equation reads

$$\int dh P(h) e^{\beta h \sum_a \sigma^a} = \exp \left\{ 3\gamma + 3\gamma \int dh_1 dh_2 P(h_1) P(h_2) G(h_1, h_2) \right\}, \quad (1.11)$$

where

$$G(h_1, h_2) = \left(\frac{\cosh(\beta(h_1 + h_2)) + e^{-2\beta} \cosh(\beta(h_1 - h_2))}{\cosh(\beta(h_1 - h_2)) + e^{-2\beta} \cosh(\beta(h_1 + h_2))} \right)^{\frac{1}{2} \sum_a \sigma^a}. \quad (1.12)$$

In the case of *satisfiable* $hSAT$, at $\beta \rightarrow \infty$ ($T = 0$), the spins turn out to be subject to an effective local field h which fluctuates from site to site according to the following simple probability distribution

$$P(h) = \sum_{\ell \geq 0} p_{\gamma}^{(\ell)} \delta(h - \ell) \quad (1.13)$$

in which

$$p_{\gamma}^{(\ell)} = (3\gamma)^{\ell} \frac{(1 - p_{\gamma}^{(0)})^{2\ell} p_{\gamma}^{(0)}}{\ell!} \quad (1.14)$$

and where $p_{\gamma}^{(0)} \equiv p_{\gamma}$ must satisfy a saddle-point self-consistency equation. The above structure is not surprising for a ferromagnetic model since $1 - p_{\gamma}$ is nothing but the fraction of sites which have a non vanishing field and that therefore are totally magnetized. The saddle-point equations simplify once rewritten in terms the probability distribution $P(m)$ of the local magnetizations $m_i = 0, 1$.

Following the notation without random gauge ($J_{ijk} = +1, \forall \{i, j, k\} \in E$), the $P(m)$ arising from the replica theory takes the particularly simple form,

$$P(m) = p_\gamma \delta_{m,0} + (1 - p_\gamma) \delta_{m,1}, \quad (1.15)$$

where $\delta_{\cdot,\cdot}$ is the Kronecker-symbol. Thus, a fraction $1 - p_\gamma$ of all logical variables is *frozen* to $+1$ in all ground states, whereas the others take both truth values with same frequency. The self-consistent equation for p_γ arising from Eq.(1.11),

$$p_\gamma = e^{-3\gamma(1-p_\gamma)^2} = \sum_{c=0}^{\infty} e^{-3\gamma} \frac{(3\gamma)^c}{c!} (1 - (1 - p_\gamma)^2)^c, \quad (1.16)$$

can be justified by simple probabilistic arguments: A variable is frozen if and only if it is contained in at least one hyper-edge $\{i, j, k\} \in E$ where also the two neighbors are frozen. Thus a variable is unfrozen, $m_i = 0$, if and only if every adjacent hyper-edge contains at least one more unfrozen variable. For a spin of connectivity c , this happens according to Eq.(1.15) with probability $(1 - (1 - p_\gamma)^2)^c$. The average over the Poisson-distribution $e^{-3\gamma}(3\gamma)^c/c!$ of connectivities c results in the total probability for a variable to be unfrozen, so Eq.(1.16) follows. As an additional result of replica theory, we derive the ground-state entropy

$$s(\gamma) = \lim_{N \rightarrow \infty} \frac{1}{N} \log \mathcal{N}_{gs} = \log(2) \left(p_\gamma (1 - \log p_\gamma) - \gamma [1 - (1 - p_\gamma)^3] \right). \quad (1.17)$$

For small γ , Eq.(1.16) has only the trivial solution $p_\gamma = 1$ where all variables are unfrozen, i.e. $m_i = 0$ for all i . No internal structure is found in the set of satisfying assignments and, choosing randomly two of them, they have Hamming distance $0.5N + O(\sqrt{N})$. To leading order in N , the order in the M 4-clauses sets act independently, each dividing the number of satisfying assignments by two and so $\mathcal{N}_{gs} = 2^{N(1-\gamma)}$. This is a clear sign that the structure of the hyper-graph is still tree-like.

At $\gamma_d = 0.818$, a new solution of Eq.(1.16) appears discontinuously, having a fraction $(1 - p_\gamma) = 0.712$ completely magnetized variables. This transition can be seen as a percolation transition of fully magnetized triples of connected variables. The entropy of this solution remains however smaller than the entropy $1 - \gamma$ of the paramagnetic solution, thus the total solution space is still correctly described by $m_i = 0$ for all $i = 1, \dots, N$. The appearance of the new solution signals however a structural change in the set of solutions which breaks into an exponential number of clusters. The cluster containing the imposed solution $x_i = +1$ is described by the new meta-stable solution.

Another important difference to the low- γ phase is an exponential number of local minima of the energy function (2.4) showing up at γ_d . These have positive energies, and the corresponding logical assignments do not satisfy the hSAT formula. Algorithms which decrease the energy in every time step by local variable changes, like e.g. zero-temperature Glauber dynamics or greedy algorithms, get

almost surely trapped in these states and do not find a zero-energy ground state for $\gamma > \gamma_d$. Randomized algorithms may escape from these minima, but as found numerically, this causes a polynomial slowing down.

Above γ_d increasing γ , the number of ground-state clusters decreases. At $\gamma_c = 0.918$ all but one ground-state clusters disappear, and the non-trivial solution of (1.16) becomes the stable one. So only the cluster including the imposed solution survives, it still contains $2^{0.082N}$ solutions, but 88.3% of all variables are fixed to +1, thus forming the *backbone* which appears discontinuously. As is known from Ref. [7], the existence of an extensive backbone is closely related to the exponential computational hardness of a problem. The remaining 11.7% of unfrozen variables change their values from ground-state to ground-state. They are contained in small disconnected components or dangling ends of the hyper-graph.

The behavior of frustrated hSAT is similar, as given both by numerical analysis and by RS or variational RSB calculations. We find that the solution $x_i = +1$ (and its corresponding cluster) in satisfiable hSAT are just superimposed to the solution structure of random hSAT. Thus, the statistical properties of the solutions do not change for $\gamma < \gamma_c$, including also the clustering of solutions above γ_d . At $\gamma_c = 0.918$ the model undergoes a SAT/UNSAT transition, and the solution entropy jumps from 0.082 down to minus infinity. The variational RSB calculation gives a value for the dynamical critical connectivity $\gamma_{d,rsb}^{var} \simeq 0.83$ which is close to the exact value 0.818. This result gives evidence for the validity of the variational approach in the region where local minima first appear, i.e. where the result does not depend strongly on the specific functional Ansatz made for the RSB probability distributions. For the SAT/UNSAT static transition the predictions of the variational RSB analysis can be strongly affected by the restriction of the functional space which does not necessarily match the geometrical structure (clustering) of the space of solution. However, in the case of hSAT the results are still in good agreement, we find $\gamma_{c,rsb}^{var} \simeq 0.935$.

1.5 Connection with graph theory

In the hSAT model, we are able to extract exact results – without the need of RSB – by identifying the topological structures in the underlying hyper-graph which are responsible of the SAT/UNSAT transition (or of frustration and glassiness). The presence (or the absence) of such topological structures in the hyper-graph drastically changes the statistical mechanical properties of the model. The different phase transitions can be viewed as different kinds of percolation in the random graph theory language [49].

We have already seen that the formation at $\gamma_d = 0.818$ of a locally stable ferromagnetic state in the unfrustrated hSAT can be understood in term of percolation arguments. The same arguments reveal that at γ_d many metastables states arise in both versions of the model, giving rise to a dynamical transition.

In order to understand what happens at the critical point γ_c we need to introduce the notion of *hyper-loop*, that is the most natural generalization of the usual *loop* to graphs where multi-vertices links are allowed. Given a random graph $\mathcal{G} = (V, E)$, where V is the set of vertices and E is the set of (hyper-)links, a hyper-loop can be defined as a non-zero set of (hyper-)links, $R \subset E$, such that the degree of the subgraph $\mathcal{L} = (V, R)$ is even, i.e. every vertex belongs to an even number of (hyper-)links (including zero). In Fig. 1.1 (left) we show the smallest hyper-loop in a $K = 3$ random hyper-graph. Note that in random hyper-graph typical hyper-loops are very large and the one shown in Fig. 1.1 (left) is extremely rare for N large.

In a similar way we can identify those vertices which are totally constrained. A set of (hyper-)links, $T^{(i)} \subset E$, constrains completely the spin at site i if in the sub-graph $\mathcal{F} = (V, T^{(i)})$ the vertex i has an odd degree and the remaining vertices an even one. In Fig. 1.1 (right) we show the smallest of such structures.

In a configuration whose energy is zero (SAT assignment) we have that $S_i S_j S_k = J_{ijk}, \forall \{i, j, k\} \in E$. Then, given any hyper-loop R , we have that

$$\prod_{\{i,j,k\} \in R} J_{ijk} = \prod_{\{i,j,k\} \in R} S_i S_j S_k = 1 \quad , \quad (1.18)$$

where the second equality comes from the fact that in the second product every spin appears an even number of times.

In the frustrated hSAT the coupling are randomly fixed to ± 1 and, consequently, the first product in Eq.(1.18) is equal to -1 with probability 1/2. Then we can conclude that as soon as one hyper-loop arises in the hyper-graph half the formulæ become unsatisfiable. In general, given a hyper-graph with N_{hl} hyper-loops, the fraction of SAT formulæ (with that given hyper-graph) is $2^{-N_{hl}}$. Still one needs to average this fraction over the random hyper-graph in order to obtain the right fraction of SAT formulæ.

We have numerically found that at the critical value $\gamma_c = 0.918$ the percolation of hyper-loops takes place, that is, in the large N limit, the average number of hyper-loops $N_{hl}(\gamma)$ is zero for $\gamma < \gamma_c$ and $\mathcal{O}(N)$ for $\gamma > \gamma_c$. This is the direct explanation of the SAT/UNSAT transition in terms of hyper-graph topology.

In the unfrustrated model $J_{ijk} = 1$ and Eq.(1.18) is always satisfied. However, the mean number of hyper-loops $N_{hl}(\gamma)$ is related to the entropy of the satisfiable hSAT through $S(\gamma) = \log(2)(1 - \gamma + N_{hl}(\gamma)/N)$. The derivation of this equality straightforward if we consider the linear system modulo 2 of M equations in N variables, introduced at the end of section 2.2. In terms of the linear system hyper-loops represents combination of equations giving a trivial one (e.g. $0 = 0$) which does not fix any degree of freedom. The entropy, which is proportional to the number of degree of freedom, is then given by $S(\gamma) = \log(2)(N - M - N_{hl}(\gamma))/N$.

Considering now a totally constrained spin at site ℓ and a SAT assignment,

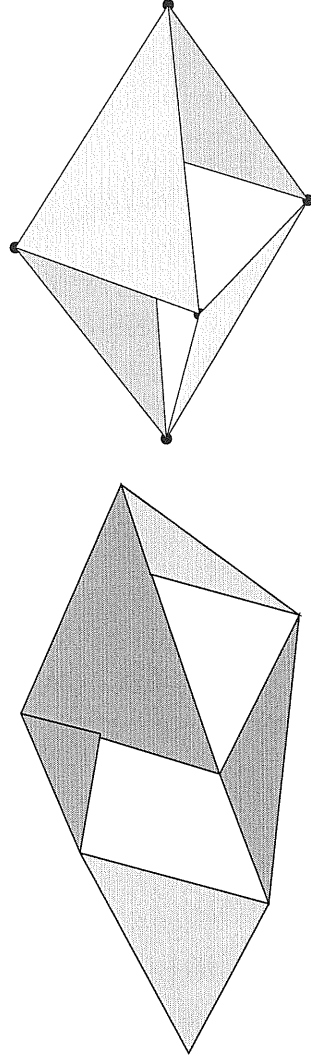


Figure 1.1: The simplest hyper-loop (above) and the hyper-loop with one totally constrained vertex of odd degree (below) [30]. Triangles represent the interaction between the three spins located at the vertices. The black dot represents the constrained spin residing on the odd-degree vertex of the hyper-loop.

we have that

$$\prod_{\{i,j,k\} \in T^{(\ell)}} J_{ijk} = \prod_{\{i,j,k\} \in T^{(\ell)}} S_i S_j S_k = S_\ell \quad . \quad (1.19)$$

Then, in every SAT formula, hyper-loops with one odd-degree vertex (to be denoted by the label $hl - 1$) fix one spin variable to a complicated function of the couplings. We have numerically checked, that such structures arise at γ_c , like hyper-loops, but in a discontinuous way.

In the satisfiable hSAT we have that $J_{ijk} = 1$, so that any independent hyper-loop with one odd degree vertex fixes one spin to 1 [31]. Then the magnetization of the model is equal to the mean density of such loops, $m(\gamma) = \rho_{hl-1}(\gamma) = N_{hl-1}(\gamma)/N$. Because of the discontinuous nature of the transition the limits $\lim_{\gamma \rightarrow \gamma_c^-} \rho_{hl-1}(\gamma) = 0$ and $\lim_{\gamma \rightarrow \gamma_c^+} \rho_{hl-1}(\gamma) = m_c = 0.883$ do not coincide.

In the frustrated hSAT Eq.(1.19) fixes the variables belonging to the backbone. Then one would be tempted to relate the backbone size to the density $\rho_{hl-1}(\gamma)$ of hyper-loops with one frozen vertex (which is true) and to estimate the backbone size at the critical point to be 88.3% (which is not true). Indeed at the critical point there is a coexistence of SAT and UNSAT formulæ (see next section) and for $\gamma > \gamma_c$ all the formulæ become UNSAT in the large N limit. Then Eq.(1.19) can be applied only for $\gamma < \gamma_c$ where the density ρ_{hl-1} goes to zero when $N \rightarrow \infty$. While the appearance of the backbone is necessarily related to the presence of hyper-loops with frozen vertices, the estimation of its size is non-trivial. A very rough estimate can be obtained assuming that at the critical point half the formulæ are SAT (according to the numerical results presented in the next section) and that the backbone size is 0 for UNSAT formulæ and 0.88 for SAT ones. Under these very crude hypothesis the backbone size would be 0.44, which is not too far from the numerical result (see next section).

1.6 Numerical results

We have performed extensive numerical experiments on both versions of hSAT in order to confirm analytical predictions and to compute quantities which are not accessible analytically. Beside the $GF[2]$ polynomial method, we have also used two local algorithms, namely the Davis-Putnam (DP) complete backtrack search [27] and the incomplete walk-SAT randomized heuristic search [22], to check the hardness of the problem for local search. The existence of at least one solution in the satisfiable hSAT allowed us to run walk-SAT in the whole range of γ , the halting criterion always being finding a SAT assignment.

The first set of results concerns the numerical determinations of the critical points of hSAT obtained by the polynomial method over large samples.

For the frustrated case, the fraction of satisfiable instances drops down to zero at $\gamma_c = 0.918$. In Fig. 1.2 we show this fraction as a function of γ , which has been obtained, for any size N , counting the number of hyper-loops in 10^4

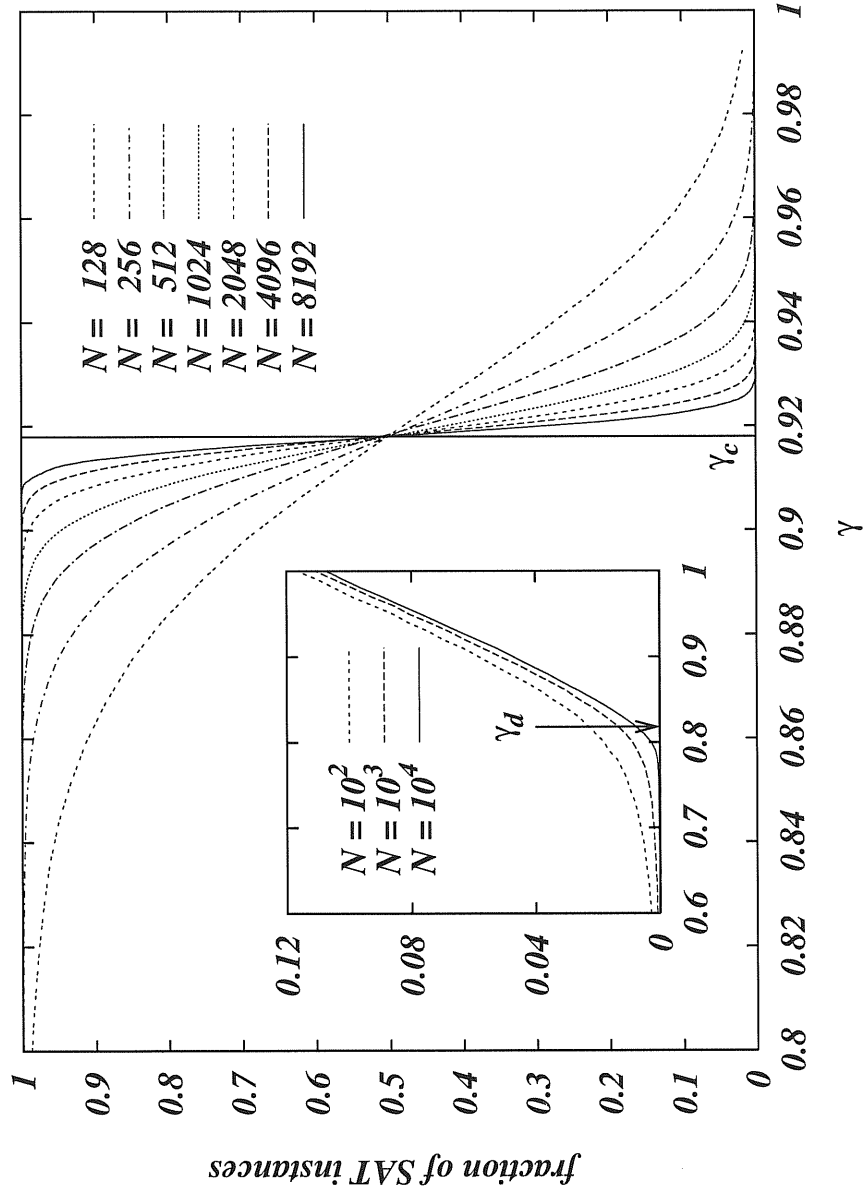


Figure 1.2: The probability that a formula is SAT as a function of the coupling density. Inset: The energy reached by a deterministic rule becomes different from zero at the dynamical critical point.

different random hyper-graphs. For any given random hyper-graph the fraction of SAT formulæ is given by $2^{-N_{hl}}$, where $N_{hl}(\gamma)$ is the number of hyper-loops. The same set of simulations run on the satisfiable hSAT show that at exactly the same γ_c , the model undergoes a discontinuous ferromagnetic transition.

At $\gamma_d = 0.818$ a dynamical transition takes place in both versions of hSAT. There appears an exponentially large number of positive energy local minima strongly affecting non-randomized dynamics, which is not able to overcome energy barriers. We can easily detect the dynamical transition by adopting the following deterministic algorithm as a probe and by checking where it stops converging to solutions. The algorithm exploits the only local source of correlations among variables that is fluctuations in connectivity. At each step, the algorithm chooses the variable with highest connectivity, fixes its value at random and it simplifies the formula (“unit clause propagation” [27]). As can be seen in the inset of Fig. 1.2 the energy reached running the above process on very large formulæ ($N = 10^2, 10^3, 10^4$) starts to deviate from zero at a value which is highly compatible with the analytical prediction $\gamma_d = 0.818$. Unfortunately the mathematical analysis of this kind of algorithm appears to be beyond our present skills due to the correlations induced into the simplified formulæ by the particular choice of variables. For a simple random (connectivity independent) choice of the variable the algorithm can be analyzed along the lines of Ref. [32] and a convergence can be proved up to $\gamma = 2/3$, which is also a rigorous lower bound to the true critical density γ_c . A rigorous upper bound is easily established by noticing that the probability for the satisfiability of a formula at fixed γ is bounded by the number of satisfying assignments, averaged over all formulæ of length γN . It follows $\gamma_c < 2 \log 2$ (which is the so called *annealed* bound known in the statistical mechanics of disordered media).

We have performed standard finite size scaling analysis in order to determine the size of the critical window $w(N)$ and the ν exponent defined by $w(N) \propto N^{-1/\nu}$ for large N .

As soon as in a growing random hyper-graph the first hyper-loop arises the fraction of SAT formulæ drops down to 0.5. We have measured the mean γ value where this event takes place, $\gamma_c(N)$. Such value scales as $\gamma_c(N) - \gamma_c \propto N^{-1}$, i.e. its critical exponent is $\nu = 1$ as expected for a discontinuous transition (see lower inset in Fig. 1.3).

However in the model there is also another source of pure statistical (not critical) fluctuations [33]. These fluctuations come from the fact that almost every formula can be modify by the addition (or deletion) of order \sqrt{N} clauses without changing its satisfiability. Therefore in the large N limit these purely statistical fluctuations will dominate the critical ones, leading to an exponent $\nu = 2$ in the scaling of the SAT probability. In the upper inset in Fig. 1.3 we show the width of the critical region [34] as a function of N , together with the best fit of the kind $Ax^{-B} + Cx^{-1/2}$. Notably the best fitting value for B is perfectly compatible with 1, giving more evidence to the crossover from critical

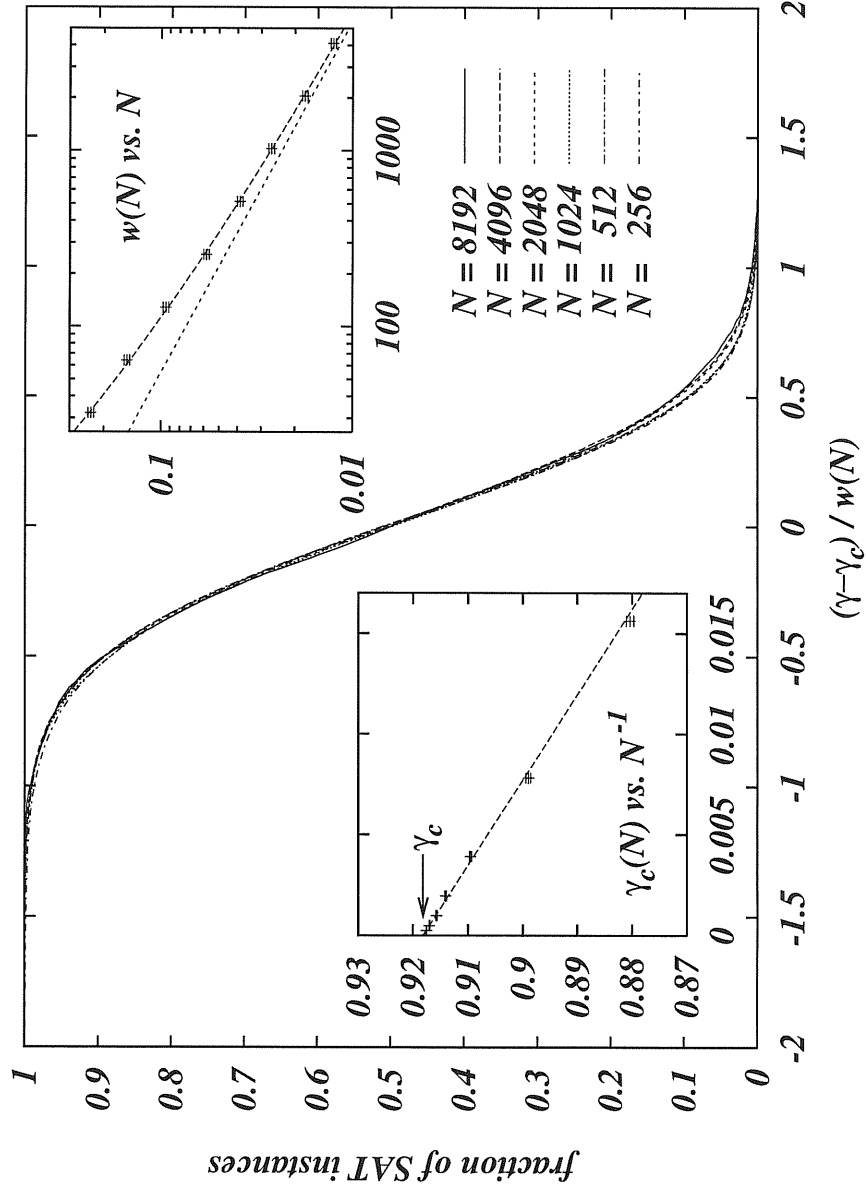


Figure 1.3: Scaling function for the SAT probability. Lower inset: The γ value where the first hyper-loop arises scales as N^{-1} . Upper inset: The critical width undergoes a crossover from $\nu = 1$ to $\nu = 2$. The fitting curve is $3.4/N + 0.74/\sqrt{N}$, while the line is the asymptote $0.74/\sqrt{N}$.

fluctuations ($\nu = 1$) to statistical ones ($\nu = 2$).

In the main part of Fig. 1.3 we show the scaling function for the SAT probability. Note that the value at criticality is equal to 0.5 up to the numerical precision. Slight deviations from perfect scaling appear in the $\gamma > \gamma_c$ region. However scaling relations hold only close to the critical point and our data perfectly collapse in all the range where the SAT probability is between 0.2 and 0.8.

The different kind of transition taking place at γ_c in the two versions of hSAT is reflected in the behavior of their entropies $s(\gamma)$ shown in Fig. 1.4 and defined as the normalized logarithm of the number of assignments minimizing the energy. For $\gamma \leq \gamma_c$ both entropies coincide and they have the analytical expression $s(\gamma) = \log(2)(1 - \gamma)$ up to γ_c . For $\gamma > \gamma_c$, while the entropy of the satisfiable hSAT decreases exponentially fast with γ (the solutions are more and more concentrated around the superimposed one), in the frustrated version the entropy decreases more slowly with γ , indicating that the number of unsat assignments minimizing the energy remains exponentially large up to $\gamma \gg \gamma_c$.

At the SAT/UNSAT transition the solution space acquires a backbone structure, with a finite fraction of the variables that take the same value in all the solutions. Above the critical threshold a similar structure characterizes the ground states. In the inset of Fig. 1.4 we report the results of exhaustive ground states enumeration on small systems, giving the average size of the backbone and the average energy. Increasing the system size, the average energy converges to zero for $\gamma < \gamma_c$ and it becomes positive at γ_c in a continuous way. In the UNSAT region, even for small sizes N , the energy slope rapidly converges to the value $1/8$ which is the analytical prediction in the large γ limit. The appearance of the backbone becomes sharper increasing the system size and, in the thermodynamical limit ($N \rightarrow \infty$), we expect it to be zero for $\gamma < \gamma_c$ and finite for $\gamma \geq \gamma_c$, consistently with a random first order phase transition predicted by the replica theory. As can be seen in the inset of Fig. 1.4 the backbone size does not depend strongly on the system size in the UNSAT phase. As discussed in Ref. [7] the presence of a finite backbone is conjectured to be the source of computational hardness in finding solutions at the SAT/UNSAT transition for both complete and randomized local algorithms.

In the $\gamma > \gamma_c$ region the backbone size shows clear oscillations, due to finite size effects. At fixed energy the backbone size is a non-decreasing function of γ , but it typically decreases when the energy jumps to a higher value. For finite systems such jumps, which are of order $1/N$, are particularly evident and induce observable fluctuations in the backbone. We expect these fluctuations to disappear in the thermodynamic limit.

In the satisfiable hSAT once we consider only the lowest local minima configurations just above the zero energy solutions (the so called *excited states*) we find that they share completely the same statistical properties with the ground states of the corresponding frustrated hSAT, i.e. the model defined over the same

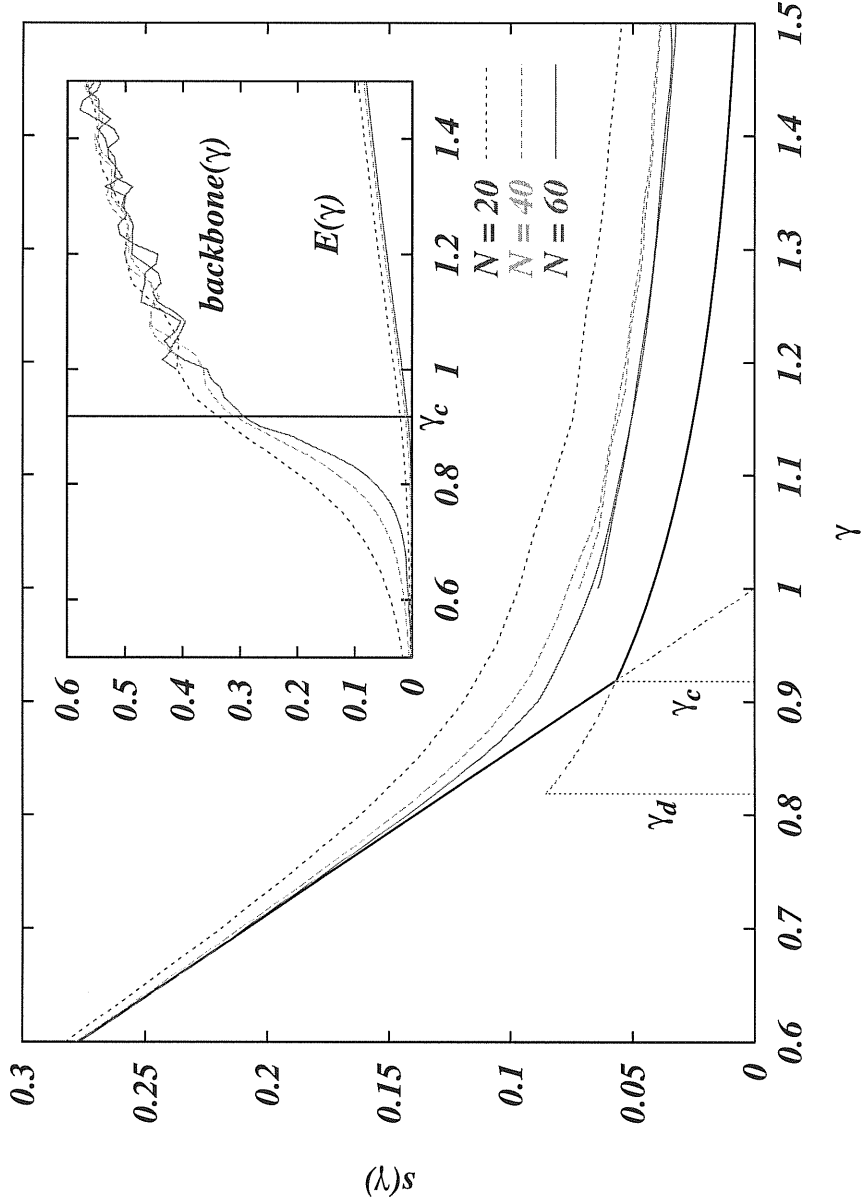


Figure 1.4: The lowest lines are the analytical expressions for the entropy of the unfrustrated model. The numerical estimation (not reported) perfectly coincide. Dashed parts correspond to metastable states. The rest of the data (entropy in the main body and energy and backbone size in the inset) come from exhaustive enumeration of the ground states in the frustrated model and of first excited states in the unfrustrated one (only $N = 40, 60$) and they coincide.

random hyper-graph with randomized couplings. We have performed a set of DP runs in satisfiable hSAT similar to the ones used previously, with the additional requirement of not considering the superimposed solution. The backbone size, the average energy and the entropy of the excited states just above the solution are identical to those measured on the ground states of the frustrated version (see Fig. 1.4). These results, together with some preliminary analytical findings [35], show in detail why a model without quenched frustration behave and can be modeled as having random sign interactions, i.e. like a spin glass model. Such a mapping is believed to play a particularly important role in spin glass theory of structural glasses, in which the only source of frustration is geometrical (i.e. dynamical). Once the Boltzmann temperature T is introduced in the model, the critical points of hSAT can be thought of as zero temperature limits of critical lines in the (T, γ) plane. In spite of the absence of any static frustration and of the existence of a pure “crystalline” state (the spin configurations corresponding to the satisfying assignment), the spin system undergoes several dynamical and static transitions as the temperature is lowered. Both the crystalline state and the first excited states are never reached in any sub-exponential time and the system stays for very large times in the metastable states (the same happens in the frustrated version).

In Fig. 1.5 we report data concerning the computational costs for finding a solution in the satisfiable hSAT and for proving satisfiability for the frustrated hSAT [36]. For both algorithms (DP and walk-SAT) and in the whole range of γ , we have measured the logarithm of the running time averaged over thousands of samples of different sizes. The choice of analyzing the averaged logarithm instead of the logarithm of the average is dictated by the presence of fat tails in the running time distributions, even in the $\gamma < \gamma_c$ region. The averaged logarithm provides directly the information on the most probable cost.

The main body of the figure displays the DP computational costs for proving satisfiability in h-SAT and for finding the satisfying assignment in the satisfiable h-SAT (given the same underlying hyper-graph structure). Both costs show a sharp easy-hard transition at γ_c , where an enormous increase in the typical running times take place. For $\gamma < \gamma_c$ both costs obviously coincide and they increase as a power law of N , the only effect of γ_d being a change of the exponent from 1 to a large value which eventually diverges at γ_c . For $\gamma > \gamma_c$, the computational costs remain very high, i.e. $\langle \log[\tau(\gamma)] \rangle \propto \sigma(\gamma)N$, with an exponent σ slowly decreasing as $1/\gamma$ [37].

In the inset of Fig. 1.5 we show the average logarithm of the running times needed by walk-SAT for finding a solution in the satisfiable hSAT model. Analogously to DP the walk-SAT costs undergo an easy-hard transition at γ_c . Interestingly enough, above γ_c the computational costs for finding solutions remains quite high and they do not decrease as in DP, where the additional constraints act as a pruning strategy in the search process. In the hard satisfiable region standard heuristic algorithms, like walk-SAT, get stuck in local minima and they are not

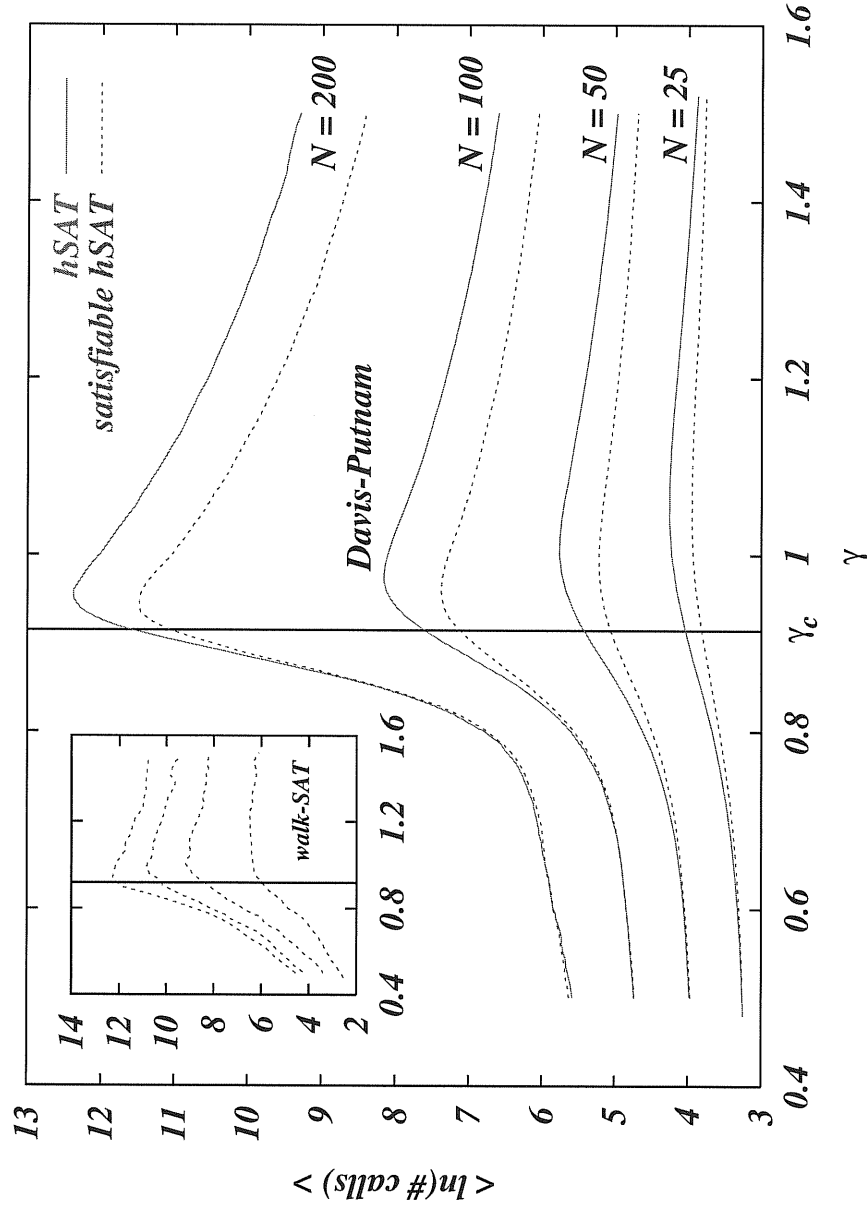


Figure 1.5: The computational costs for finding a solution or proving unsatisfiability with the Davis-Putnam algorithm strongly increase approaching the critical point. For $\gamma \geq \gamma_c$ they grow exponentially with the problem size N . Inset: The same computational costs for the walk-SAT algorithm, which can be run for every γ in the satisfiable model ($N = 25, 50, 75, 100$).

able to exploit the large number of constraints in order to reduce the searching space. In particular, the large scale structure ($O(N)$) of the hyper-loops makes them difficult to detect in polynomial time by a local search process which is dominated by the exponential branching process arising at each step when the tentative choices for the variables are made. However, having at hand a model on which new heuristic algorithms can be tested, such a searching optimization can be hopefully pushed far forward.

A thorough analysis of computational costs dependence on system size N gives the following overall picture. For $\gamma \leq \gamma_d$ the cost is a linear function of N . For $\gamma \in [\gamma_d, \gamma_c)$ the typical cost increases as a power law of N , with an exponent which should diverge in γ_c . For $\gamma \geq \gamma_c$ the costs are exponential in N .

1.7 Conclusions

part we have presented the study of a model for the generation of random combinatorial problems, called hyper-SAT. In the context of Theoretical Computer Science such a model is simply the completely balanced version of the famous K-SAT model, while in Statistical Physics it corresponds to a diluted p-spin model at zero temperature. We have studied two version of the model, a frustrated one and an unfrustrated one.

Increasing the density of interactions, $\gamma = M/N$, the model undergoes two transitions. A first one purely dynamical and a second static one. Such phase transitions have a straightforward interpretation in terms of the structure of the underlying hyper-graphs, leading to a very simple connection between Theoretical Computer Science and Graph Theory, and Statistical Physics of random systems.

The locations of phase boundaries, can be computed exactly within the RS replica formalism, leading to $\gamma_d = 0.818$ and $\gamma_c = 0.918$. We expect the replica results to be computable also by more rigorous probabilistic methods.

Exploiting a global method for solving the problems which is polynomial in the problem size we have been able to study very large problems, determining with high precision critical points and critical exponent and a cross-over from critical fluctuations to statistical ones has been measured.

We have found that the computational costs for finding a solution to a typical problem or to prove that it is unsatisfiable using only local search methods undergoes an easy-hard transitions at γ_d and γ_c . The growth of the costs with the problem size N is linear up to γ_d , is polynomial in N in the range $\gamma_d \leq \gamma \leq \gamma_c$ and finally it becomes exponential in N above γ_c . The above scenario has been checked for both complete and incomplete local algorithms, thanks to the existence of an halting criterion in the unfrustrated version of hyper-SAT where at least one solution is guaranteed to exist. The use of this model as a benchmark for heuristic algorithms may result in a good improvement of their performances in the phase where many local minima are present.

h-SAT can be viewed as an intermediate model between 2-SAT and K-SAT ($K > 2$), which is exactly solvable and in which the presence of hidden solutions can be kept under some control. Hopefully, some of the results and methods of our analysis of h-SAT can be extended to NP-complete problems.

Chapter 2

The 2+p-XOR-SAT variant

2.1 Introduction: the role of phase coexistence and finite-size scaling

In this chapter we study a mixed version of the previous problem, where sentences made out of 2 (2-XOR-SAT) and 3 (3-XOR-SAT) variables are mixed with relative probability p . Rare events are shown to affect the combinatorial “phase diagram” leading to a coexistence of solvable and unsolvable instances of the combinatorial problem in a certain region of the parameters characterizing the model. Such instances differ by a non-extensive quantity in the ground state energy of the associated diluted spin-glass model. We also show that the critical exponent ν , controlling the size of the critical window where the probability of having solutions vanishes, depends on the model parameters, shedding light on the link between random hyper-graph topology and universality classes. In the case of random satisfiability, a similar behavior was conjectured to be connected to the onset of computational intractability.

The statistical mechanics study of random K -SAT have provided some geometrical understanding of the onset of complexity at the phase transition through the introduction of a functional order parameter which describes the geometrical structure of the space of solutions. The nature of the SAT/UNSAT transition for the different values of K appears to be a particularly relevant prediction [7]. The SAT/UNSAT transition is accompanied by a smooth (respectively abrupt) change in the structure of the solutions of the 2-SAT (resp. 3-SAT) problem. More specifically, at the phase boundary a finite fraction of the variables become fully constrained while the entropy density remains finite. Such a fraction of frozen variables (i.e. those variables which take the same value in all solutions) may undergo a continuous (2-SAT) or discontinuous (3-SAT) growth at the critical point. This discrepancy is responsible for the difference of typical complexities of both models recently observed in numerical studies. The typical solving time of search algorithms displays an easy-hard pattern as a function of γ with a peak

of complexity close to the threshold. The peak in search cost seems to scale polynomially with N for the 2-SAT problem and exponentially with N in the 3-SAT case. From an intuitive point of view, the search for solutions ought to be more time-consuming in presence of a finite fraction of fully quenched variables since the exact determination of the latter requires an almost exhaustive enumeration of their configurations.

To test this conjecture, a mixed $2 + p$ -model has been proposed, including a fraction p (resp. $1 - p$) of clauses of length two (resp. three) and thus interpolating between the 2-SAT ($p = 0$) and 3-SAT ($p = 1$) problems. The statistical mechanics analysis predicts that the SAT/UNSAT transition becomes abrupt when $p > p_0 \simeq 0.4$ [7, 41, 42, 43]. Precise numerical simulations support the conjecture that the polynomial/exponential crossover occurs at the same critical p_0 . Though the problem is both critical ($\gamma_c = 1/(1 - p)$ for $p < p_0$) and NP-complete for any $p > 0$, it is only when the phase transition becomes of the same type of the 3-SAT case that hardness shows up. An additional argument in favor of this conclusion is given by the analysis of the finite-size effects on $P_N(\gamma, K)$ and the emergence of some universality for $p < p_0$. A detailed account of these findings may be found in [7, 41, 42, 43, 44]. For $p < p_0$ the exponent ν , which describes the shrinking of the critical window where the transition takes place, is observed to remain constant and close to the value expected for 2-SAT. The critical behavior is the same of the percolation transition in random graphs (see also ref. [45]). For $p > p_0$ the size of the window shrinks following some p -dependent exponents toward its statistical lower bound [33] but numerical data did not allow for any precise estimate.

In this paper, we study an exactly solvable version of the random 2+p SAT model which displays new features and allows us to settle the issue of universality of the critical exponents. The threshold of the model can be computed exactly as a function of the mixing parameter p in the whole range $p \in [0, 1]$. Rare events are found to be dominant also in the low γ phase, where a coexistence of satisfiable and unsatisfiable instances is found.

The existence of a global – polynomial time – algorithm for determining satisfiability allows us to perform a finite size scaling analysis around the exactly known critical points over huge samples and to show that indeed the exponent controlling the size of the critical window ceases to maintain its constant value $\nu = 3$ and becomes dependent on p as soon as the phase transition becomes discontinuous, i.e. for $p > p_0 = .25$. Above p_0 and below $p_1 \sim 0.5$, the exponent ν takes intermediate values between 3 and 2. Finally, above p_1 the critical window is determined by the statistical fluctuations of the quenched disorder [33] and so $\nu = 2$.

2.2 Model definition and outline of some results

The model we study can be viewed as the mixed $2 + p$ extension of the 3-*hyper-SAT* (hSAT) model discussed previously, as much as the $2 + p$ -SAT [7] is an extension of the usual K-SAT model. In computer science literature the hSAT model is also named XOR-SAT and its critical behavior is considered an open issue [46]. Given a set of N Boolean variables $\{x_i = 0, 1\}_{i=1, \dots, N}$ we can write an instance of our model as follows. Firstly we define the elementary constraints (a mixture of 4 and 2-clauses sets with 50% satisfying assignments):

$$\begin{aligned} C(ijk|+1) &= (x_i \vee x_j \vee x_k) \wedge (x_i \vee \bar{x}_j \vee \bar{x}_k) \\ &\quad \wedge (\bar{x}_i \vee x_j \vee \bar{x}_k) \wedge (\bar{x}_i \vee \bar{x}_j \vee x_k) \\ C(ijk|-1) &= (\bar{x}_i \vee \bar{x}_j \vee \bar{x}_k) \wedge (\bar{x}_i \vee x_j \vee x_k) \\ &\quad \wedge (x_i \vee \bar{x}_j \vee x_k) \wedge (x_i \vee x_j \vee \bar{x}_k) , \end{aligned} \quad (2.1)$$

for the 3-hSAT part, and

$$\begin{aligned} C(ij|+1) &= (x_i \vee \bar{x}_j) \wedge (\bar{x}_i \vee x_j) \\ C(ij|-1) &= (x_i \vee x_j) \wedge (\bar{x}_i \vee \bar{x}_j) , \end{aligned} \quad (2.2)$$

for the 2-hSAT part. A more compact definition can be achieved by the use of the exclusive OR operator \oplus , e.g. $C(ijk|+1) = x_i \oplus x_j \oplus x_k$. Then, we randomly choose two independent sets E_3 and E_2 of pM triples $\{i, j, k\}$ and $(1 - p)M$ couples $\{i, j\}$ among the N possible indices and respectively pM and $(1 - p)M$ associated unbiased and independent random variables $T_{ijk} = \pm 1$ and $J_{ij} = \pm 1$, and we construct a Boolean expression in Conjunctive Normal Form (CNF) as

$$F = \bigwedge_{\{i,j,k\} \in E_3} C(ijk|T_{ijk}) \bigwedge_{\{i,j\} \in E_2} C(ij|J_{ij}) . \quad (2.3)$$

As in [?], we can build a *satisfiable* version of the model choosing clauses only of the $C(ij|+1)$ and $C(ijk|+1)$ type. For $p < p_0$ the problem is easily solved by local and global algorithms, whereas interesting behaviors are found for $p > p_0$, where the local algorithms fail.

The above combinatorial definition can be recast in a simpler form as a minimization problem of a cost-energy function on a topological structure which is a mixture of a random graph (2-spin links) and hyper-graph (3-spin hyper-links). We end up with a diluted spin model where the Hamiltonian reads

$$H_J[\mathbf{S}] = M - \sum_{\{i,j,k\} \in E_3} T_{ijk} S_i S_j S_k - \sum_{\{i,j\} \in E_2} J_{ij} S_i S_j , \quad (2.4)$$

where the S_i are binary spin variables and the the random couplings can be either ± 1 at random. The satisfiable version is nothing but the ferromagnetic model: $T_{ijk} = 1$ and $J_{ij} = 1$ for any link.

As the average connectivity γ of the underlying mixed graph grows beyond a critical value $\gamma_c(p)$, the *frustrated* model undergoes a phase transition from a mixed phase in which satisfiable instances and unsatisfiable ones coexist to a phase in which all instances are unsatisfiable. At the same $\gamma_c(p)$ the associated spin glass system, undergoes a zero temperature glass transition where frustration becomes effective and the ground state energy is no longer the lowest one (i.e. that with all the interactions satisfied). At the same critical point the *unfrustrated*, i.e. ferromagnetic, version undergoes a para-ferro transition, because the same topological constraints that drive the glass (mixed SAT/UNSAT to UNSAT) transition in the frustrated model are shown to be the ones responsible for the appearance of a nonzero value of the magnetization in the unfrustrated one. We shall take advantage of such coincidence of critical lines by making the analytical calculation for the simpler ferromagnetic model.

Moreover, the nature of the phase transition changes from second to random first order, when p crosses the critical value $p_0 = 1/4$. For $p > p_0$ the critical point $\gamma_c(p)$ is preceded by a dynamical glass transition at $\gamma_d(p)$ where ergodicity breaks down and local algorithms get stuck (local algorithms are procedures which update the system configuration only by changing a finite number of variable at the same time, e.g. all single or multi spin flip dynamics, together with usual computer scientists heuristic algorithms). The dynamical glass transition exist for both versions of the model [47] and corresponds to the formation of a locally stable ferromagnetic solution in the unfrustrated model [48] (the local stability is intimately related to the ergodicity breaking).

2.3 Statistical mechanics analysis

We compute the free energy of the model with the replica method, exploiting the identity $\log \ll Z^n \gg = 1 + n \ll \log Z \gg + O(n^2)$. The n^{th} moment of the partition function is obtained by replicating n times the sum over the spin configurations and then averaging over the quenched disorder

$$\ll Z^n \gg = \sum_{\mathbf{S}^1, \mathbf{S}^2, \dots, \mathbf{S}^n} \ll \exp \left(-\beta \sum_{a=1}^n H_J[\mathbf{S}^a] \right) \gg, \quad (2.5)$$

Since each of the M clauses is independent, the probability distributions of the ferromagnetic couplings can be written as

$$\begin{aligned} P(\{T_{ijk}\}) &= \prod_{i < j < k} \left[\left(1 - \frac{6\gamma p}{N^2} \right) \delta(T_{ijk}) + \frac{6\gamma p}{N^2} \delta(T_{ijk} - 1) \right] \\ P(\{J_{ij}\}) &= \prod_{i < j} \left[\left(1 - \frac{2\gamma(1-p)}{N} \right) \delta(J_{ij}) + \frac{2\gamma(1-p)}{N} \delta(J_{ij} - 1) \right], \quad (2.6) \end{aligned}$$

giving the following expression for the $\ll Z^n \gg$:

$$\sum_{S_i^1, S_i^2, \dots, S_i^n} \exp \left\{ -\beta\gamma Nn - \gamma N + \frac{p\gamma}{N^2} \sum_{ijk} e^\beta \sum_a S_i^a S_j^a S_k^a + \frac{(1-p)\gamma}{N} \sum_{ij} e^\beta \sum_a S_i^a S_j^a + O(1) \right\} \quad (2.7)$$

Introducing the occupation fractions $c(\vec{\sigma})$ (fraction of sites with replica vector $\vec{\sigma}$), one gets

$$\begin{aligned} -\beta F[c] = & -\gamma(1 + \beta n) - \sum_{\vec{\sigma}} c(\vec{\sigma}) \log c(\vec{\sigma}) + (1-p)\gamma \sum_{\vec{\sigma}, \vec{\rho}} c(\vec{\sigma}) c(\vec{\rho}) e^\beta \sum_a \sigma^a \rho^a \\ & + p\gamma \sum_{\vec{\sigma}, \vec{\rho}, \vec{\tau}} c(\vec{\sigma}) c(\vec{\rho}) c(\vec{\tau}) e^\beta \sum_a \sigma^a \rho^a \tau^a . \end{aligned} \quad (2.8)$$

In the thermodynamic limit we can calculate the free energy via the saddle point equation obtaining

$$\begin{aligned} c(\vec{\sigma}) = & \exp \left\{ -\Lambda + 2(1-p)\gamma \sum_{\vec{\rho}} c(\vec{\rho}) \exp(\beta \sum_a \sigma^a \rho^a) \right. \\ & \left. + 3p\gamma \sum_{\vec{\rho}, \vec{\tau}} c(\vec{\rho}) c(\vec{\tau}) \exp(\beta \sum_a \sigma^a \rho^a \tau^a) \right\} \end{aligned} \quad (2.9)$$

The Lagrange multiplier $\Lambda = -\gamma(2 + p)$ ensures the normalization constraint $\sum_{\vec{\sigma}} c(\vec{\sigma}) = 1$ in the limit $n \rightarrow 0$. Finding the minimal (zero in the *unfrustrated* case) value of the cost function amounts to studying the $\beta \rightarrow \infty$ (zero temperature) properties of the model. In the Replica Symmetric (RS) Ansatz, the behavior of the spin magnetization can be described in terms of effective fields $m = \tanh \beta h$ whose probability distribution is defined through

$$c(\vec{\sigma}) = \int_{-\infty}^{\infty} dh P(h) \frac{e^{\beta h \sum_a \sigma^a}}{(2 \cosh(\beta h))^n} . \quad (2.10)$$

In the *unfrustrated* or *ferromagnetic* case, the $P(h)$ turns out to have the following simple form

$$P(h) = \sum_{l \geq 0} r_l \delta(h - l) , \quad (2.11)$$

where the effective fields only assume integer values. In the *satisfiable* model the saddle point equations all collapse in one single self-consistency equation for r_0 :

$$\begin{aligned} r_0 = & e^{-3p\gamma(1-r_0)^2 - 2(1-p)\gamma(1-r_0)} \\ = & \sum_{c_1=0}^{\infty} \sum_{c_2=0}^{\infty} e^{-3p\gamma} e^{-2(1-p)\gamma} \frac{(3p\gamma)_1^{c_1}}{c_1!} \frac{(2(1-p)\gamma)_2^{c_2}}{c_2!} (1 - (1-r_0)^2)^{c_1} (r_0)^{c_2} \end{aligned} \quad (2.12)$$

The equations for the frequency weights r_l with $l > 0$ follow from the one for r_0 and read

$$r_l = \frac{[3p\gamma(1-r_0)^2 + 2(1-p)\gamma(1-r_0)]^l}{l!} . \quad (2.13)$$

The previous self consistency equations for r_0 (or for the magnetization $m = 1 - r_0$) can easily be derived by the same probabilistic argument used in the pure 3-model, due to the fact that the clause independence allows to treat the graph and the hyper-graph part separately. Note that in the simple limit $p = 0$ we retrieve the equation for the percolation threshold in a random graph of connectivity γ [49],

$$1 - r_0 = e^{-2\gamma} \sum_{k=0}^{\infty} \frac{(2\gamma)^k}{k!} (1 - r_0^k) \quad . \quad (2.14)$$

Since the ground state energy of the ferromagnetic model is zero, the free energy coincides with the ground state entropy, which can be written as a function of p , r_0 and γ :

$$S(\gamma) = \log(2)[r_0(1 - \log(r_0)) - \gamma(1 - p)(1 - (1 - r_0)^2) - \gamma p(1 - (1 - r_0)^3)] \quad (2.15)$$

To find the value of the paramagnetic entropy we put ourself in the phase where all sets of 4- and 2-clauses act independently, each therefore dividing the number of allowed variables choice by two: the number of ground states will be $N_{gs} = 2^{N - p\gamma N - (1-p)\gamma N} = 2^{N(1-\gamma)}$. The resulting value of $S_{para} = (1 - \gamma) \log(2)$ coincides with the one found setting $r_0 = 1$ in Eq.(2.15). This may not be the case in more complicated models, where the ground state entropy is a complicated function of γ also for $\gamma < \gamma_c$, reflecting the fact that the magnetization probability distribution in the paramagnetic phase could be different from a single delta peak in $m = 0$.

Solving the saddle point equation for r_0 , we find that a paramagnetic solution with $r_0 = 1$ always exists, while at a value of $\gamma = \gamma_d(p)$ there appears a ferromagnetic solution in the satisfiable model. For $p = 0$, the critical value coincides as expected with the percolation threshold $\gamma_d(0) = 1/2$. As long as the model remains like 2-SAT, up to $p < p_0 = 0.25$, the threshold is the point where the ferromagnetic solution appears and also where its entropy exceeds the paramagnetic one. The critical magnetization is zero and the transition is continuous. For larger values of the control parameter p the transition becomes discontinuous. There appears a dynamical transition at $\gamma = \gamma_d(p)$ where locally stable solutions appear. At $\gamma = \gamma_c(p) > \gamma_d(p)$, the non trivial $r_0 \neq 1$ solution acquires an entropy larger than the paramagnetic one and becomes globally stable. The shape of $\gamma = \gamma_d(p)$ and $\gamma = \gamma_c(p)$ as functions of p are shown in Fig. 2.1. The inset picture shows the magnetization of the model at the points where the dynamical and the static transitions take place.

2.4 Numerical simulations

The model can be efficiently solved by a polynomial algorithm based on a representation modulo two (i.e. in Galois field $\text{GF}[2]$). If a formula can be satisfied,

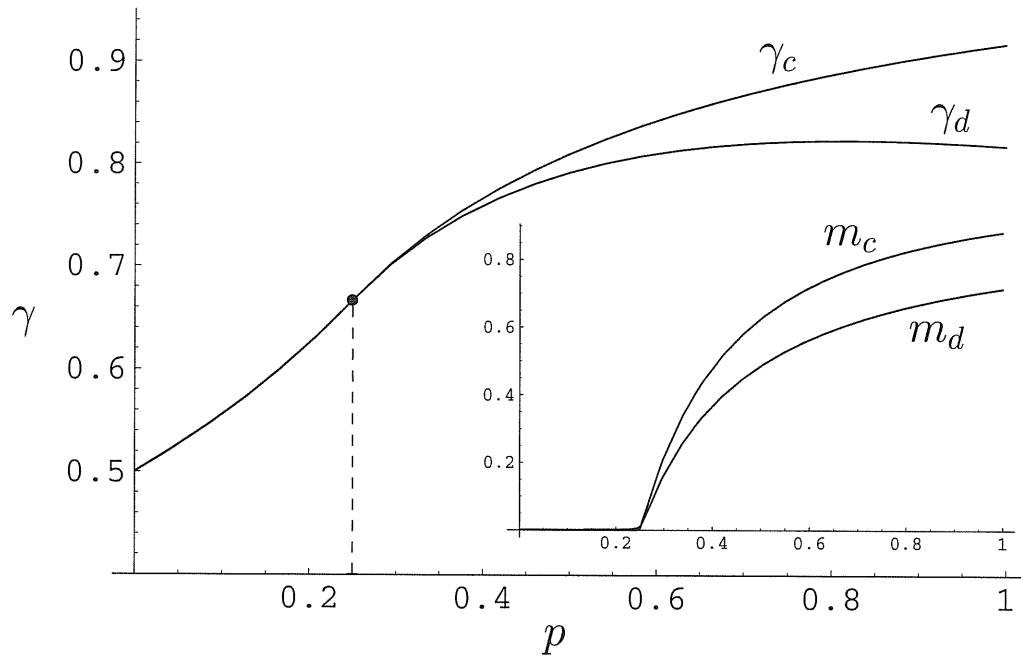


Figure 2.1: Critical lines (static and dynamic) in the (γ, p) plane. The black dot at $(0.667, 0.25)$ separates continuous transitions from discontinuous ones (where $\gamma_d < \gamma_c$). Inset: Critical magnetizations at $\gamma_d(p)$ and $\gamma_c(p)$ versus p .

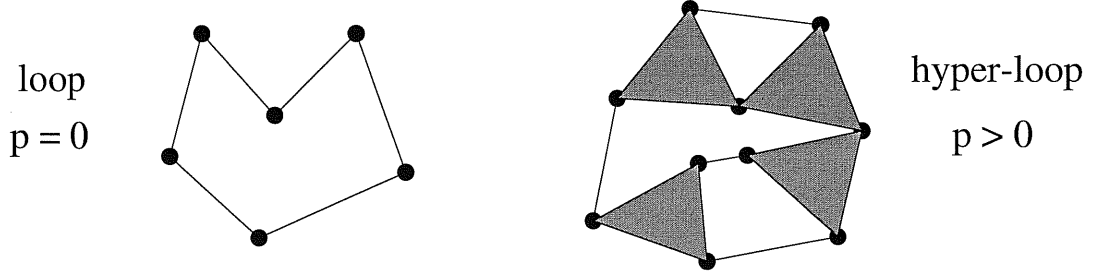


Figure 2.2: Typical loop and hyper-loop. Lines are 2-spin links, while triangles are 3-spin links. Note that every vertex has an even degree.

then a solution to the following set of M equations in N variables exists

$$\begin{cases} S_i S_j S_k = T_{ijk} & \forall \{i, j, k\} \in E_3 \\ S_i S_j = J_{ij} & \forall \{i, j\} \in E_2 \end{cases} \quad (2.16)$$

Through the mapping $S_i = (-1)^{\sigma_i}$, $J_{ij} = (-1)^{\eta_{ij}}$ and $T_{ijk} = (-1)^{\zeta_{ijk}}$, with $\sigma_i, \eta_{ijk}, \zeta_{ijk} \in \{0, 1\}$, Eq.(2.16) can be rewritten as a set of binary linear equations

$$\begin{cases} (\sigma_i + \sigma_j + \sigma_k) \bmod 2 = \zeta_{ijk} & \forall \{i, j, k\} \in E_3 \\ (\sigma_i + \sigma_j) \bmod 2 = \eta_{ij} & \forall \{i, j\} \in E_2 \end{cases} \quad (2.17)$$

For any given set of couplings $\{\eta_{ij}, \zeta_{ijk}\}$, the solutions to these equations can be easily found in polynomial time by e.g. Gaussian substitution. The solution to the M linear equations in N variables can be summarized as follows: a number N_{dep} of variables is completely determined by the values of the coupling $\{\eta_{ij}, \zeta_{ijk}\}$ and by the values of the $N_{free} = N - N_{dep}$ independent variables. The number of solutions is $2^{N_{free}}$ and the entropy $S(\gamma) = \log(2)N_{free}/N = \log(2)(1 - N_{dep}(\gamma)/N)$. As long as $N_{dep} = M$ we have the paramagnetic entropy $S_{para} = \log(2)(1 - \gamma)$. However N_{dep} may be less than M when the interactions are such that one can generate linear combinations of equations where no σ 's appear, like $0 = f(\{\eta_{ij}, \zeta_{ijk}\})$. This kind of equations correspond to the presence of loops (resp. hyper-loops) in the underlying graph (resp. hyper-graph). A hyper-loops (generalization of a loop on a hyper-graph) is defined as a set \mathcal{S} of (hyper-)links such that every spin (i.e. node) is “touched” by an even number of (hyper-)links belonging to \mathcal{S} (see Fig. 2.2).

Here we are interested in the fraction of satisfiable instances $P_{SAT}(\gamma, p)$, averaged over the random couplings distribution. One can show that, for any random (hyper-)graph, P_{SAT} is given by $2^{-N_{hl}}$, where N_{hl} is the number of independent (hyper-)loops. In Fig. 2.3 we show the fraction of satisfiable instances as a function of γ for $p = 0$ and $p = 0.5$. The vertical lines report the analytical predictions for the critical points, $\gamma_c(p = 0) = 0.5$ and $\gamma(p = 0.5) = 0.810343$.

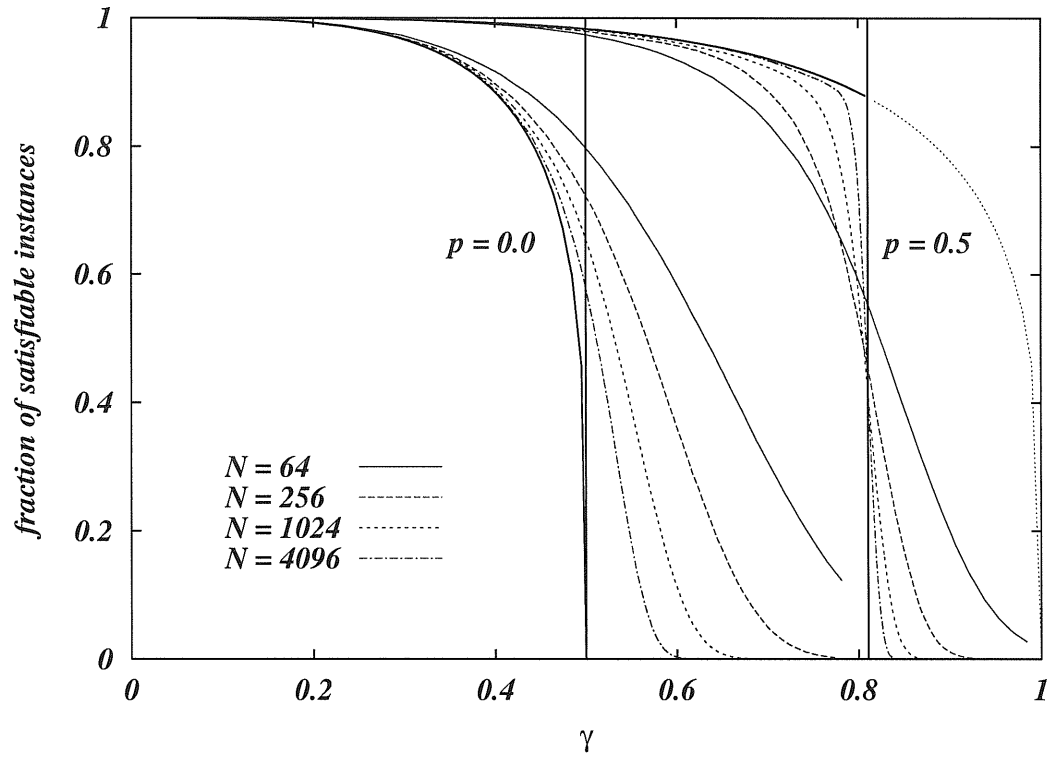


Figure 2.3: SAT probabilities $P_{SAT}(\gamma, p)$ for $p = 0$ and $p = 0.5$. Data has been averaged over 10^4 different random hyper-graphs. Vertical straight lines are analytical predictions for critical points: $\gamma_c(p = 0) = 0.5$ and $\gamma_c(p = 0.5) = 0.810343$. Bold curves for $\gamma < \gamma_c$ are analytical predictions for the SAT probability in the large N limit.

In the limit of large N and for $p = 0.5$ the fraction of SAT instances sharply vanishes at the critical point in a discontinuous way, that is $\lim_{\gamma \rightarrow \gamma_c^-} P_{SAT}(\gamma) > 0$ while $\lim_{\gamma \rightarrow \gamma_c^+} P_{SAT}(\gamma) = 0$. This is the usual behavior already measured in 3-SAT [7, 41] and 3-hyper-SAT, with the SAT probabilities measured on finite systems crossing at γ_c and becoming sharper and sharper as N increases. On the contrary for $p = 0$ and large N the probability of being SAT becomes zero at γ_c in a continuous way. The main consequence is that finite size corrections make $P_{SAT}(\gamma)$ larger than its thermodynamical limit both before and after the critical point and thus the data crossing is completely missing.

Note also that for $p < 1$ the fraction of SAT instances for $\gamma < \gamma_c(p)$ is finite and less than 1 even in the thermodynamical limit, implying a *mixed phase* of SAT and UNSAT instances. This is due to the presence in the random hypergraph of loops made only by 2-spin links (indeed the mixed phase is absent for $p = 1$ when only 3-spin interactions are allowed). The expression for the SAT probability in the thermodynamical limit (bold curves in Fig. 2.3, the lower most for $p = 0$ and the uppermost for $p = 0.5$) can be calculated analytically and the final result is

$$P_{SAT}(\gamma, p) = e^{\frac{1}{2}\gamma(1-p)[1+\gamma(1-p)]} [1 - 2\gamma(1-p)]^{1/4} \quad \text{for } \gamma \leq \gamma_c(p) \quad . \quad (2.18)$$

In order to obtain to above expression we note that the SAT probability is related to the number of (hyper-)loops by

$$P_{SAT}(\gamma, p) = \sum_{m=0}^{\infty} P(m; \gamma, p) 2^{-m} \quad , \quad (2.19)$$

where $P(m; \gamma, p)$ is the probability of having m (hyper-)loops in a random (hyper-)graph with parameters γ and p , and the factor 2^{-m} comes from the probability that for all the m (hyper-)loops the product of the interactions is 1 (thus giving no contradiction in the formula). In order to estimate $P(m; \gamma, p)$ we may restrict ourselves to consider only simple loops (made of 2-spin links), because hyper-loops which involve at least one 3-spin link are irrelevant in the thermodynamical limit. This can be easily understood with the help of the following counting argument.

The probability that a given 2-spin link is present in a random (γ, p) hypergraph is $p_2 = 2\gamma(1-p)/N$ and for a 3-spin hyper-link is $p_3 = 6\gamma p/N^2$. Thus the probability of finding in a random (γ, p) hyper-graph a hyper-loop made of n_2 links and n_3 hyper-links (n_3 must be even) is just the number of different ways one can choose the (hyper-)links times $p_2^{n_2} p_3^{n_3}$. Because the number of nodes belonging to a hyper-loop of this kind is at most $n_n = n_2 + 3n_3/2$ and the number of different hyper-loops of this kind is order N^{n_n} , we have that the probability of having a hyper-loop with n_2 links and n_3 hyper-links is order $N^{-n_3/2}$.

Then, for $\gamma < \gamma_c$ the number of hyper-loops is still finite (their number becomes infinite only at γ_c where a transition to a completely UNSAT phase takes

place) and the SAT probability, in the large N limit, is completely determined by the number of simple loops ($n_3 = 0$).

The typical number of these loops does not vanish for $\gamma < \frac{1}{2(1-p)}$, and therefore such “rare” events lead to a coexistence of SAT and UNSAT instances with equal energy density.

The average number of loops of length k can be easily calculated and it is given by $x^k/(2k)$, where $x = 2\gamma(1-p)$. The average number of loops of any size

$$A(x) = \sum_{k=3}^{\infty} \frac{x^k}{2k} = -\frac{1}{2} \ln(1-x) - \frac{x}{2} - \frac{x^2}{4} \quad , \quad (2.20)$$

indeed diverges for $x \rightarrow 1$, that is for $\gamma \rightarrow \frac{1}{2(1-p)}$. The probability of having m loops in a random (γ, p) hyper-graph is then

$$P(m; \gamma, p) = e^{-A(x)} \frac{A(x)^m}{m!} \quad , \quad (2.21)$$

and the fraction of SAT instances turns out to be the one in Eq.(2.18).

We have numerically calculated the SAT probabilities for many p and N values, finding a transition from a mixed to a completely UNSAT phase at the $\gamma_c(p)$ analytically calculated in the previous section. We also find, in agreement with analytical results, that the transition is continuous as long as $p \leq 1/4$ and then it becomes discontinuous in the SAT probability.

Let us now concentrate on the scaling with N of the critical region. We have considered several alternative definitions for the critical region. The one we present here seems to be the simplest and also the most robust, in the sense it can be safely used when the transition is both continuous ($p \leq 0.25$) and discontinuous ($p > 0.25$). We assume that the size of the critical region is inversely proportional to the derivative of the SAT probability at the critical point

$$w(N, p)^{-1} = \left. \frac{\partial P_{SAT}(\gamma, p)}{\partial \gamma} \right|_{\gamma=\gamma_c} \quad . \quad (2.22)$$

For any value of p the width $w(N)$ goes to zero for large N and the scaling exponent $\nu(p)$ is defined through

$$w(N, p) \propto N^{-1/\nu(p)} \quad . \quad (2.23)$$

In Fig. 2.4 we show, in a log-log scale, $w(N, p)$ as a function of N for many p values, together with the fits to the data. The uppermost and lowermost lines have slopes $-1/3$ and $-1/2$ respectively. Data for $p \leq 0.5$ can be perfectly fitted by simple power laws (straight lines in Fig. 2.4) and the resulting $\nu(p)$ exponents have been reported in Fig. 2.5. We note that as long as $p \leq 0.25$ the ν exponent turns out to be highly compatible with 3, which is known to be the right value

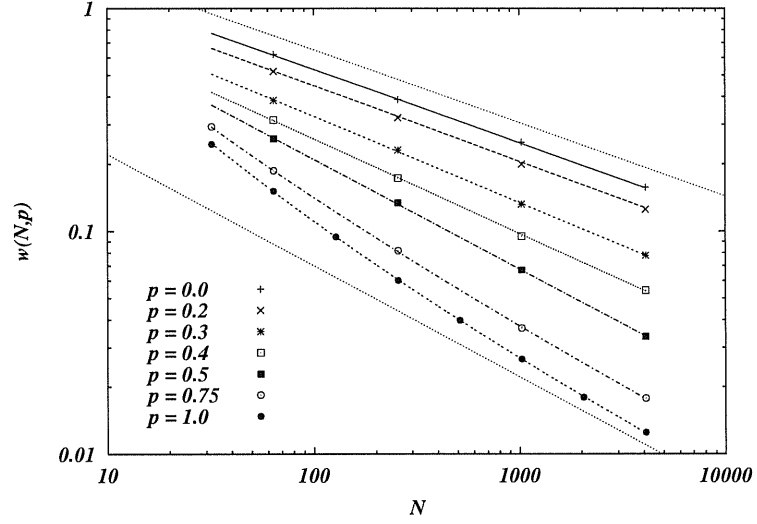


Figure 2.4: Scaling of the critical window width. Errors are smaller than symbols. Lines are fits to the data.

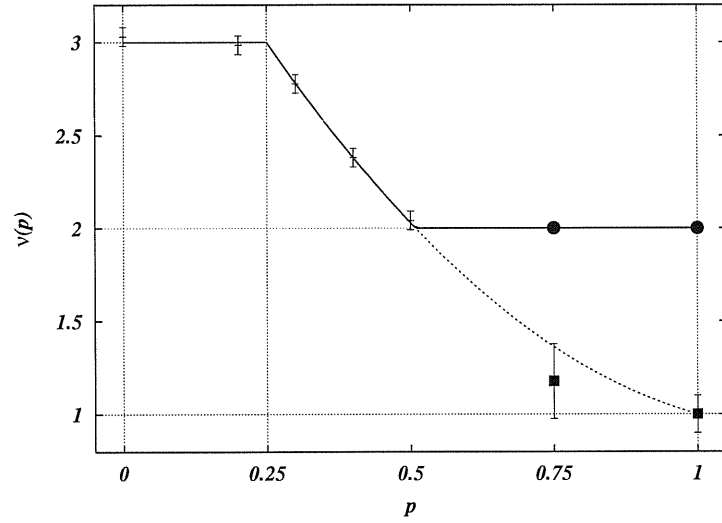


Figure 2.5: Critical ν exponents obtained from the fits shown in Fig. 2.4. For $p = 0.75$ and $p = 1$ filled squares show the subleading term power exponent, the leading term one being fixed to $-1/2$ (filled circles).

for $p = 0$. Thus we conclude that for $p < 1/4$ the exponents are those of the $p = 0$ fixed point.

For $0.25 < p \leq 0.5$ we find that the ν exponent takes non-trivial values between 2 and 3. Then one of the following two conclusions may hold. Either the transition for $p > p_0$ is driven by the $p = 1$ fixed point and the ν exponent is not universal, or more probably any different p value defines a new universality class. This result is very surprising and interesting for the possibility that different universality classes are simply the consequence of the random hyper-graph topology.

More complicated is the fitting procedure for $p > 0.5$. In a recent paper [33] Wilson has shown that in SAT problems there are intrinsic statistical fluctuations due to the way one constructs the formula. This *white noise* induces fluctuations of order $N^{-1/2}$ in the SAT probability. If critical fluctuations decay faster than statistical ones (i.e. $\nu < 2$), in the limit of large N the latter will dominate and the resulting exponent saturates to $\nu = 2$. Data for $p = 0.75$ and $p = 1$ shown in Fig. 2.4 have a clear upwards bending, which we interpret as a crossover from critical (with $\nu < 2$) to statistical ($\nu = 2$) fluctuations. Then we have fitted these two data sets with a sum of two power laws, $w(N) = AN^{-1/\nu} + BN^{-1/2}$. The goodness of the fits (shown with lines in Fig. 2.4) confirm the dominance of statistical fluctuations for large N . Moreover we have been able to extract also a very rough estimate of the critical exponent ν from the subleading term. In Fig. 2.5 we show with filled squares these values, which turn out to be more or less in agreement with a simple extrapolation from $p \leq 0.5$ results.

2.5 Conclusions and perspectives

The exact analysis of a solvable model for the generation of random combinatorial problems has allowed us to show that combinatorial phase diagrams can be affected by rare events leading to a mixed SAT/UNSAT phase. The energy difference between such SAT and UNSAT instances is non extensive and therefore non detectable by the usual $\beta \rightarrow \infty$ statistical mechanics studies. However, a simple probabilistic argument is sufficient to recover the correct proportion of instances.

Moreover, through the exact location of phase boundaries together with the use of a polynomial global algorithm for determining the existence of solutions we have been able to give a precise characterization of the critical exponents ν depending on the mixing parameter p . The p -dependent behavior conjectured in ref. [7] for the random $2+p$ SAT case finds here a quantitative confirmation. The mixing parameter dependency also shows that the value of the scaling exponents is not completely determined by the nature of the phase transition and that the universality class the transition belongs to is very probably determined by the topology of the random hyper-graph. The model we study has also a physical

interpretation as a diluted spin glass system. It would be interesting to know whether the parameter-dependent behavior of critical exponent plays any role in some physically accessible systems.

A last remark on the generalization of the present model. With the same analytical techniques presented here, one can easily solve a Hamiltonian containing a fraction f_k of k -spin interacting terms for any suitable choice of the parameters f_k [50]. The case presented in this paper ($f_2 = 1 - p$ and $f_3 = p$) is the simplest one. There are choices which show a phase diagram still more complex with, for example, a continuous phase transition preceded by a dynamical one.

Acknowledgments

Thanks to Riccardo and Federico, who taught me what I know and are both teachers and friends. To Johannes, Silvio and all Statistical Mechanics group at ICTP. To Gianluca who stood by me before and after the Master. To Mario and all my friends at SISSA. To my parents and my family, who never ask me why am I doing this. To Cecilia, so far so close.

Bibliography

- [1] Email: `riccife@ictp.trieste.it`
- [2] Email: `weigt@theorie.physik.uni-goettingen.de`
- [3] Email: `zecchina@ictp.trieste.it`
- [1] M. Garey, and D.S. Johnson, *Computers and Intractability; A guide to the theory of NP-completeness*, W.H. Freeman and Co., San Francisco, 1979;
C. Papadimitriou, *Computational Complexity*, Addison-Wesley, 1994;
- [2] S.A. Cook, *The complexity of theorem-proving procedures*, in *Proc. 3rd Ann. ACM Symp. on Theory of Computing*, Assoc. Comput. Mach., New York, 151 (1971)
- [3] Y.-T. Fu, and P.W. Anderson, in *Lectures in the Sciences of Complexity*, D. Stein (ed.), (Addison-Wesley, 1989), p. 815.
- [4] D. Mitchell, B. Selman and H. Levesque, “Hard and Easy Distributions of SAT problems,” *Proc. of Am. Assoc. for Artif. Intell. AAAI-92*, 456-465 (1992).
- [5] S. Kirkpatrick and B. Selman, *Science* **264**, 1297 (1994)
- [6] Issue 1–2, *Artificial Intelligence* **81**, T. Hogg, B. A. Huberman, and C. Williams, Eds., (1996)
- [7] R. Monasson, R. Zecchina, S. Kirkpatrick, B. Selman, L. Troyansky, *Nature* **400**, 133 (1999)
- [8] M. Weigt, A. K. Hartmann, *Phys. Rev. Lett.* **84**, 6118 (2000)
- [9] D. Achlioptas, C. Gomes, D. Liang, H. Kautz, B. Selman, “Generating Satisfiable Problem Instances”, preprint.
- [10] B. Bollobás, C. Borgs, J.T. Chayes, J.H. Kim, D.B. Wilson, `arXiv:math.CO/9909031` .

- [11] A. Goerdt, in *Proc. 7th Int. Symp. on Mathematical Foundations of Computer Science*, 264 (1992); *Journal of Computer and System Sciences*, **53**, 469 (1996)
V. Chvátal and B. Reed, in *Proc. 33rd IEEE Symp. on Foundations of Computer Science*, 620 (1992)
- [12] B. Aspvall, M.F. Plass and R.E. Tarjan, *Inf. Process. Lett.* **8**, 121 (1979)
- [13] M. Mézard, G. Parisi, M.A. Virasoro, *Spin Glass Theory and Beyond*, World Scientific, Singapore, 1987
- [14] D. Gross, M. Mézard, *Nuclear Phys. B* **240**, 431 (1984)
- [15] E. Gardner, *Nucl. Phys. B* **257**, 747 (1985)
- [16] E. Gardner and B. Derrida, *J. Phys. A* **22**, 1983 (1989)
- [17] T.R. Kirkpatrick and D. Thirumalai, *Phys. Rev. Lett.* **58**, 2091 (1987)
- [18] A. Barrat, R. Zecchina, *Phys. Rev. E* **59**, 1299 (1999)
- [19] In this context, the study of Boolean satisfiability (K-SAT) problems has played a major role, allowing for both theoretical and numerical analysis. An instance of random K-SAT consists of a set of $M = \alpha N$ random logical clauses over N Boolean variables. Each clause contains exactly K variables which are connected by logical OR operations and appear negated with probability $1/2$. The important computational question is whether there exists an assignment to the variables that simultaneously satisfies all clauses (“constraints”) for a given instance. When α crosses a critical value $\alpha_c(K)$ and for $N \gg 1$, the probability of finding solutions vanishes abruptly, i.e. $\alpha_c(K)$ identifies the so called satisfiable to unsatisfiable (SAT/UNSAT) transition. At the same point and for $K \geq 3$, hard computational instances cluster, leading to an exponential median search cost for the most efficient known algorithms. The random K-SAT problem therefore provides a good model for the study of the onset of true intractability of “typical” instances of NP-complete problems. Moreover, recent results [7] have pointed out a clear connection between typical-case computational complexity and the type of threshold phenomena taking place at $\alpha_c(K)$.
- [20] Similarly to the hSAT model, also random K-SAT can be mapped onto a minimization problem of a spin cost function. Keeping the same definition of the spin variables one can construct a function which counts the number of violated clauses. In the $K = 3$ case such a function reads

$$H[\Delta, S] = \frac{\alpha}{8}N - \sum_{i=1}^N H_i S_i + \sum_{i < j} T_{ij} S_i S_j - \sum_{i < j < k} J_{ijk} S_i S_j S_k \quad , \quad (2.24)$$

where the couplings are given by $H_i = \frac{1}{8} \sum_{\ell=1}^M \Delta_{\ell i}$, $T_{ij} = \frac{1}{8} \sum_{\ell=1}^M \Delta_{\ell i} \Delta_{\ell j}$ and $J_{ijk} = \frac{1}{8} \sum_{\ell=1}^M \Delta_{\ell i} \Delta_{\ell j} \Delta_{\ell k}$. The random parameters $\Delta_{\ell i}$ take the value 1 (resp. -1) if the variable x_i (resp. \bar{x}_i) appears in the ℓ -th clause, and 0 otherwise. Comparison of the above expression with Eq.(2.4) clarifies the difference with hSAT in which only the 3-spin interaction term appears.

- [21] D. Achlioptas, “Setting two variables at a time yields a new lower bound for random 3-SAT”, preprint.
- [22] B. Selman, H.A. Kautz, B. Cohen, “Local search strategies for satisfiability testing”, in *DIMACS* (1993)
- [23] J.M. Crawford and L.D. Auton, “Experimental results on the cross-over point in satisfiability problems.” *Proc. AAAI-93*, Washington, DC, 21–27 (1993).
- [24] The Boolean expressions which are generated in this way are simply those which have the highest probability given the satisfying assignment and therefore are those with maximum entropy, i.e. the easiest to satisfy!
- [25] G. Biroli, R. Monasson, M. Weigt, *Europ. Phys. J.*, **B 14**, 551 (2000)
- [26] However the entropy is not trivially given by $\log(2)$ times the fraction of variables which do not belong to the backbone.
- [27] M. Davis, H. Putnam, *J. Assoc. Comput. Mach.*, **7** (1960), 201–215.
- [28] R. Monasson and R. Zecchina, *Phys. Rev. Lett.* **76**, 3881 (1996); *Phys. Rev. E* **56**, 1357 (1997).
- [29] B. Bollobás, “Random Graphs”, (Academic Press, London, 1985).
- [30] Note that in random hyper-graphs the probability that any pair of vertices belongs to more than one hyper-link is proportional to $1/N$ for large N , then we have not considered this possibility when constructing the structures in Fig. 1.1.
- [31] Taking also the gauge into account we have $J_{ijk} = \varepsilon_i \varepsilon_j \varepsilon_k$ and the constraint becomes $S_\ell = \varepsilon_\ell$.
- [32] M.-T. Chao, J. Franco, *Inform. Sci.* **51**, 289 (1990)
- [33] D.B. Wilson, preprint arXiv:math/0005136.
- [34] The size of the critical window has been estimated as the inverse of the derivative at γ_c of the curves in Fig. 1.2. Other methods give compatible results.

- [35] J. Berg, S. Franz, M. Leone, F. Ricci-Tersenghi and R. Zecchina, work in progress.
- [36] In any SAT phase proving satisfiability is equivalent to finding a ground state whereas in an UNSAT phase the proof of unsatisfiability does not provide any information on the precise assignments of the variables in the ground states.
- [37] Similarly to what happens in Max-KSAT. See for instance, “On the Complexity of Unsatisfiability Proofs for Random k -CNF Formulas”, P. Baume, R. Karp, T. Pitassi and M. Saks, *Proc. STOC-98*, 561-571 (1998);
- [38] *Artif. Intel.* **81**, issues 1–2 (1996).
- [39] D. Mitchell, B. Selman, and H. Levesque, in *Proceedings of the Tenth National Conference on Artificial Intelligence (AAAI-92)* (AAAI Press, Menlo Park, CA, 1992), p. 459.
- [40] special issue on *NP-hardness and Phase Transitions*, O. Dubois, R. Monasson, B. Selman and R. Zecchina, *Theoretical Computer Science* in press.
- [41] R. Monasson, R. Zecchina, S. Kirkpatrick, B. Selman and L. Troyansky, *Random Structures and Algorithms* **3**, 414 (1999).
- [42] R. Monasson and R. Zecchina, *J. Phys. A* **31**, 9209 (1998).
- [43] G. Biroli, R. Monasson, M. Weigt, *Eur. Phys. J. B* **14**, 551 (2000).
- [44] R. Monasson and R. Zecchina, *Phys. Rev. Lett.* **76**, 3881 (1996); *Phys. Rev. E* **56**, 1357 (1997).
- [45] B. Bollobás, C. Borgs, J.T. Chayes, J.H. Kim and D.B. Wilson, preprint [arXiv:math.CO/9909031](https://arxiv.org/abs/math.CO/9909031).
- [46] N. Creignou and H. Daude, *Discr. Appl. Math.* **96–97**, 41 (1999).
- [47] S. Franz, M. Mézard, F. Ricci-Tersenghi, M. Weigt and R. Zecchina, preprint [cond-mat/0103026](https://arxiv.org/abs/cond-mat/0103026).
- [48] S. Franz, M. Leone, F. Ricci-Tersenghi and R. Zecchina, in preparation.
- [49] B. Bollobás, *Random Graphs* (Academic Press, London, 1985).
- [50] M. Leone, F. Ricci-Tersenghi and R. Zecchina, in preparation.